

Garwood Valley, Antarctica: A new record of Last Glacial Maximum to Holocene glaciofluvial processes in the McMurdo Dry Valleys

Joseph S. Levy^{1,†}, Andrew G. Fountain², Jim E. O'Connor³, Kathy A. Welch⁴, and W. Berry Lyons⁴

¹College of Earth, Ocean, and Atmospheric Sciences, Oregon State University, Corvallis, Oregon 97331, USA

²Department of Geology, Portland State University, Portland, Oregon 97201, USA

³U.S. Geological Survey Oregon Water Science Center, Portland, Oregon 97201, USA

⁴The School of Earth Sciences and Byrd Polar Research Center, Ohio State University, Columbus, Ohio 43210, USA

ABSTRACT

We document the age and extent of late Quaternary glaciofluvial processes in Garwood Valley, McMurdo Dry Valleys, Antarctica, using mapping, stratigraphy, geochronology, and geochemical analysis of sedimentary and ice deposits. Geomorphic and stratigraphic evidence indicates damming of the valley at its Ross Sea outlet by the expanded Ross Sea ice sheet during the Last Glacial Maximum. Damming resulted in development of a proglacial lake in Garwood Valley that persisted from late Pleistocene to mid-Holocene time, and in the formation of a multilevel delta complex that overlies intact, supraglacial till and buried glacier ice detached from the Ross Sea ice sheet. Radiocarbon dating of delta deposits and inferred relationships between paleolake level and Ross Sea ice sheet grounding line positions indicate that the Ross Sea ice sheet advanced north of Garwood Valley at ca. 21.5 ka and retreated south of the valley between 7.3 and 5.5 ka. Buried ice remaining in Garwood Valley has a similar geochemical fingerprint to grounded Ross Sea ice sheet material elsewhere in the southern Dry Valleys. The sedimentary sequence in Garwood Valley preserves evidence of glaciofluvial interactions and climate-driven hydrological activity from the end of the Pleistocene through the mid-Holocene, making it an unusually complete record of climate activity and paleoenvironmental conditions from the terrestrial Antarctic.

INTRODUCTION

The McMurdo Dry Valleys of Antarctica preserve an ~14-m.y.-old record of the complex interactions between glaciations and the land

surface (Sugden et al., 1993). Determining the dynamics of ice-sheet advance and retreat in Antarctica during the Pleistocene-Holocene transition has become a topic of interest because of its potential for informing predictions of ice-sheet response to future episodes of warming (Conway et al., 1999). The McMurdo Dry Valleys are an ideal environment in which to date the record of Last Glacial Maximum (LGM) ice-sheet processes because, while they are currently ice-sheet free, the McMurdo Dry Valleys preserve glacial drift and till units from multiple glacial periods and from multiple ice-sheet sources (including both East and West Antarctic Ice Sheets) (Brook et al., 1995; Denton et al., 1989; Hall and Denton, 2000; Stuiver et al., 1981).

In order for glacial till and/or stranded glacier ice to be deposited within the McMurdo Dry Valleys, the Ross Ice Shelf (Fig. 1), fed by the East and West Antarctic Ice Sheets, must have been thicker during glacial periods. In particular, the ice sheet needs to have been grounded (here, referred to as the Ross Sea ice sheet when in a grounded state) with sufficient thickness to drive ice flow upslope into the McMurdo Dry Valleys (Stuiver et al., 1981).

Direct dating of glacial tills can be challenging in the absence of exogenous markers like volcanic ash (e.g., Marchant et al., 2002). Consequently, research in the Ross Sea region and Transantarctic Mountains has focused primarily on dating the lacustrine effects of ice sheets—the formation of lakes and their deposits during times when valley mouths were blocked by the expanded Ross Sea ice sheet (e.g., Clayton-Greene et al., 1988; Conway et al., 1999; Dage, 1985; Denton et al., 1989; Hall and Denton, 2000; Hall et al., 2000a, 2002; Hendy et al., 1979; Péwé, 1960; Prentice et al., 2008; Stuiver et al., 1981)—and the isostatic responses—marine shell deposits uplifted by isostatic rebound postglaciation (Hall et al., 2000a). This first dating strategy largely relies on dating algal mats and lacustrine carbonates

from fluvial deltas perched on valley walls. The lake levels required to have formed these deltas are higher than the overflow heights for modern McMurdo Dry Valleys closed basin lakes (Doran et al., 1994). Accordingly, for the elevated deltas and shorelines to have formed, the grounding line for the Ross Sea ice sheet must have been north of the McMurdo Dry Valleys, allowing the ice sheet to plug the lower ends of the valleys, resulting in the formation of glacier-dammed lakes. For the lakes to have drained, the grounding line must have retreated south of the McMurdo Dry Valleys, allowing local base level to return to sea level (Stuiver et al., 1981).

This glacial dam model has motivated extensive mapping and dating of shorelines and paleolake delta deposits in the McMurdo Dry Valleys in order to decipher the late Quaternary history of the Ross Sea ice sheet. Pleistocene and Holocene paleolakes have been mapped using this method in the northern McMurdo Dry Valleys: Taylor Valley (Hall and Denton, 2000; Hall et al., 2000a; Hendy et al., 1979; Higgins et al., 2000), Wright Valley (Hall and Denton, 2005), Victoria Valley (Hall et al., 2002); and in the southern McMurdo Dry Valleys abutting the Royal Society range: Marshall Valley (Dage, 1985) and Miers Valley (Clayton-Greene et al., 1988). Notably, Garwood Valley (Figs. 1 and 2), located north of Marshall and Miers Valleys, has not been mapped in detail, although deltaic deposits were observed by Péwé (1960), who named the paleolake inferred to have produced the deposits “Glacial Lake Howard.” Interestingly, Hendy (2000) reported that no evidence had yet been identified supporting the existence of an LGM-age paleolake dammed by the Ross Sea ice sheet in Garwood Valley, suggesting that delta deposits identified by Péwé (1960) in Garwood Valley are likely of Holocene, rather than late Pleistocene, age (Hendy, 2000; Stuiver et al., 1981).

Here, we report on the stratigraphy of recently exposed glaciofluvial deposits on the floor of Garwood Valley, Antarctica (Figs. 2 and 3). We show that the Garwood Valley paleolake and

[†]Present address: Institute for Geophysics, University of Texas, Austin, Texas 78758-4445, USA. E-mail: joe.levy@utexas.edu.

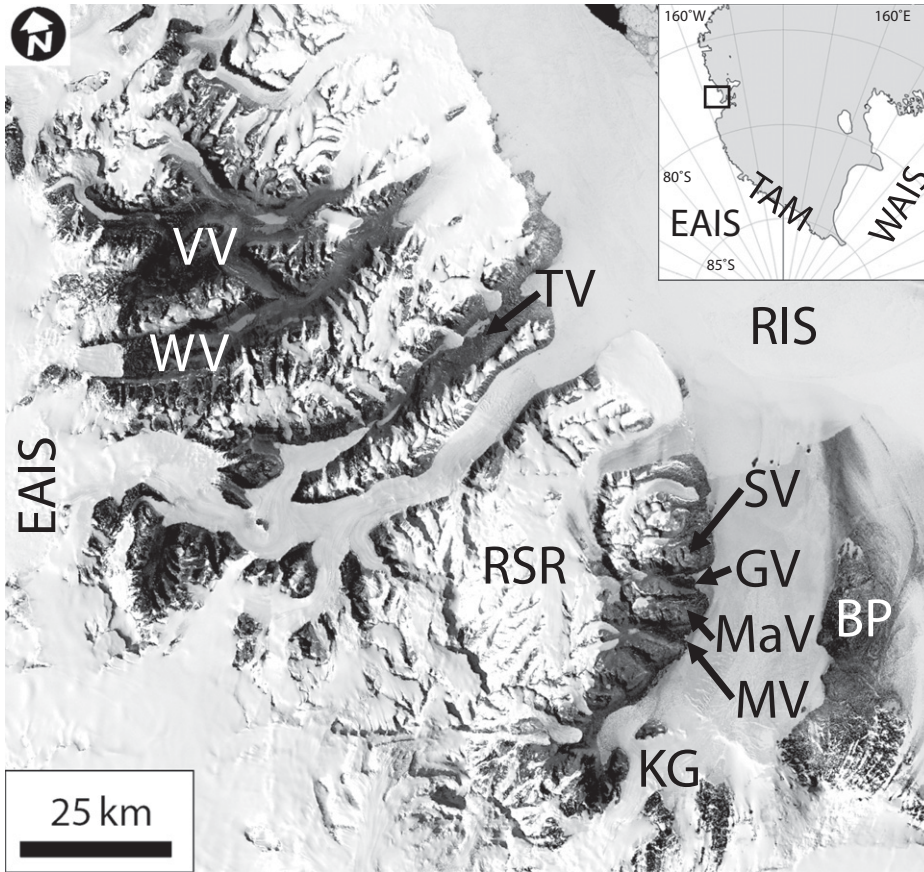


Figure 1. Context map showing the location of Garwood Valley (GV) in the McMurdo Dry Valleys, Antarctica. Base map is LIMA Landsat image mosaic (Bindschadler et al., 2008). TV—Taylor Valley, VV—Victoria Valley, WV—Wright Valley, MV—Miers Valley, EAIS—East Antarctic Ice Sheet, WAIS—West Antarctic Ice Sheet, TAM—Trans-Antarctic Mountains, RSR—Royal Society Range, SV—Salmon Valley, MaV—Marshall Valley, BP—Brown Peninsula, RIS—Ross Ice Shelf, and KG—Koettlitz Glacier. Inset map shows the location of the McMurdo Dry Valleys (box).

delta deposits are unusual in the McMurdo Dry Valleys in that they span the complete sequence from ice damming of Garwood Valley, through paleolake growth and decay, to modern-climate modification processes in a single outcrop. They preserve ice and sediments that can be geochemically correlated with Ross Sea ice sheet material and proglacial lake sediments collected from neighboring valleys. From stratigraphic interpretation and dating of these deposits, we infer the glaciofluvial processes and the climate conditions in the McMurdo Dry Valleys during the transition out of the LGM. In particular, we test the working hypothesis that, during the LGM, a tongue of the grounded Ross Sea ice sheet entered Garwood Valley, producing a glacier-dammed lake that drained or dried out several times, and that ultimately, the grounded ice in the valley became decoupled from the Ross Sea ice sheet and ablated in place, becoming mantled with ablation till and eolian sediments.

GEOLOGICAL CONTEXT

Garwood Valley (78.026°S, 164.144°E) is a coastal Dry Valley located between the Royal Society Range and the Ross Sea, west of the Brown Peninsula (Figs. 1 and 2). The valley extends ~13 km from its head in the Shangri-La region adjacent to the Joyce Glacier east to its mouth at the shore of the Ross Sea. At its widest, Garwood Valley is ~3.5 km across and has a steep-walled, U-shaped cross section. Surface elevations on the valley floor range between sea level and ~400 m, while the valley is bounded by ridges that approach elevations of ~1000 m, separating it from Marshall Valley (to the south) and Salmon Valley (to the north). The Garwood Glacier is located ~8 km inland from the coast, at an elevation of ~200 m, and it divides the valley into upper and lower sections. Here, we report on glaciofluvial features in the lower portion of the

valley between the modern Garwood Glacier and the Ross Sea.

Regionally, the bedrock underlying the southern McMurdo Dry Valleys (Salmon, Garwood, Marshall, Miers) is composed of Skelton Group metasediments and igneous intrusives of Precambrian to Cambrian age (Dagel, 1985). The Royal Society Range that forms the head of Garwood Valley is composed of Devonian to Triassic Beacon Supergroup sandstones, intruded by sills of the Ferrar Dolerite (Dagel, 1985).

Glaciologically, Garwood Valley has been affected both by local alpine glaciers, such as the Garwood, Joyce, and nearby Koettlitz Glaciers, as well as by the East/West Antarctic Ice Sheet or Ross Sea ice sheet invading up the valley from the Ross Sea. At least two distinct widespread tills are present above 500 m in the lower valley, dated by cosmogenic methods to 272 ± 7 ka and 104 ± 3 ka (Brook et al., 1995). These old till ages are interpreted to reflect inheritance of cosmogenic nuclides from till parent rocks, or to represent tills emplaced by grounded ice during the preceding glacial periods (Brook et al., 1995). Initial observations by Péwé (1960) of the glaciofluvial deposits along the valley floor (those analyzed here) led him to infer glaciation of Garwood Valley by an expanded lobe of the nearby Koettlitz Glacier at ca. 6 ka.

Regionally, the presence of porphyritic anorthoclase phonolite (“kenyte”) in the widely distributed (and commonly ice-cored) Ross I drift unit, which fringes the coastal margin of the McMurdo Dry Valleys from Taylor south to Miers (Stuiver et al., 1981), has led to a broad consensus that the source of this glacial deposit was Ross Sea ice sheet material that transported Ross Archipelago volcanics (typified by “kenyte” from Ross Island) to the south and west. On the basis of radiocarbon-dated algal mats, lake carbonates, and marine mollusks associated with glaciofluvial features related to this ice advance, the Ross Sea ice sheet grounded in the McMurdo Dry Valleys ca. 28,860 ^{14}C yr B.P. (Denton et al., 1989; Denton and Marchant, 2000; Hall and Denton, 2000; Stuiver et al., 1981), or slightly later (ca. 18–22 ka; Joy et al., 2011) as the ice sheet advanced. The grounding line for the Ross Sea ice sheet is thought to have returned south of the McMurdo Dry Valleys by 6500 ^{14}C yr B.P. (Conway et al., 1999; Denton et al., 1989; Hall and Denton, 2000; Stuiver et al., 1981). The recession date is inferred, in part, from dating of two algal mat samples collected within the glacial till deposit at the mouth of Garwood Valley (see next section) dated to 6190 ± 80 and 6580 ± 50 ^{14}C yr B.P. (Stuiver et al., 1981). In subsequent sections, we integrate our

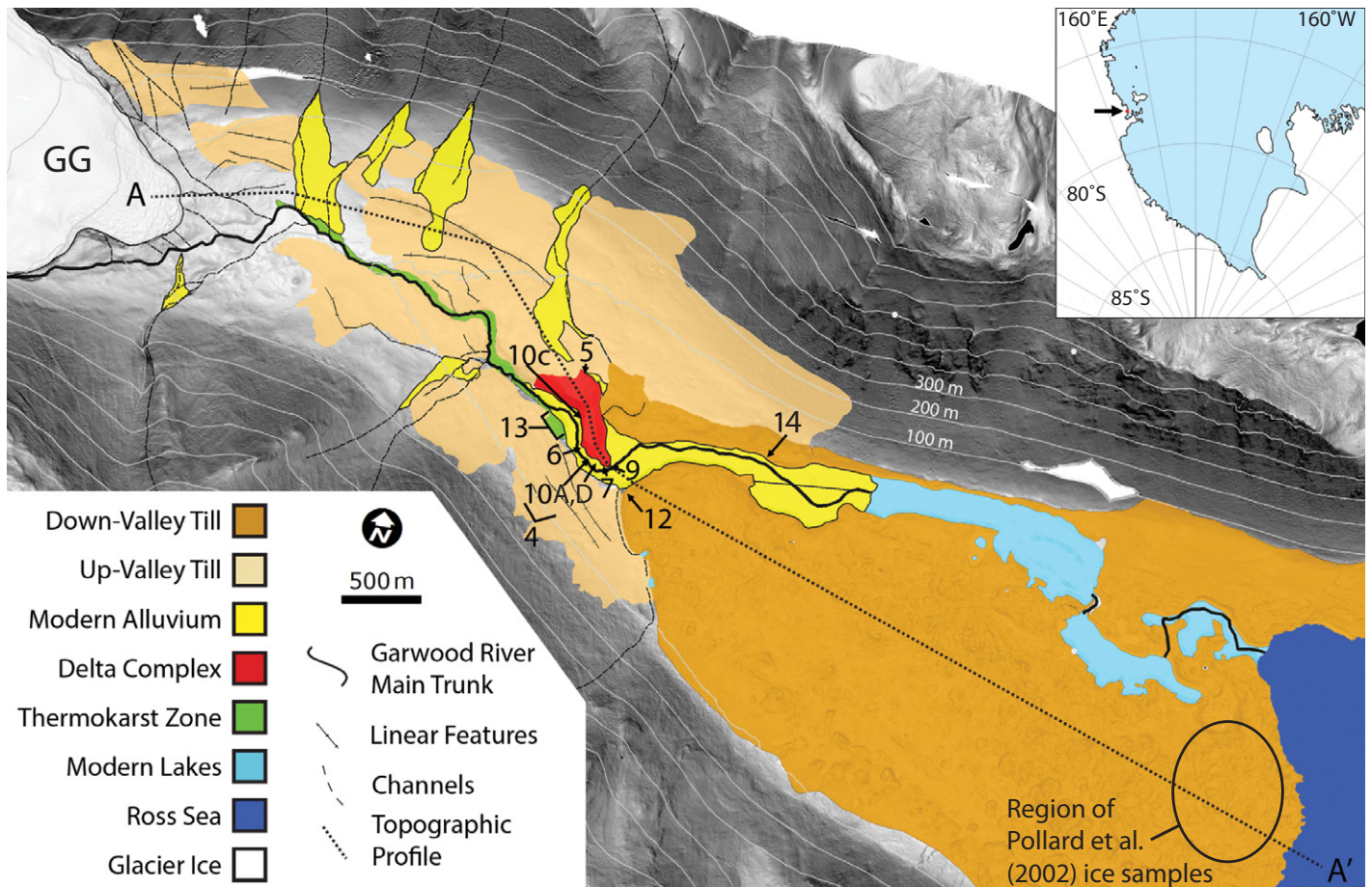


Figure 2. Context map showing Garwood Valley surface units and figure locations. Inset shows the Ross Sea region, the southern McMurdo Dry Valleys (arrow), and the location of Garwood Valley (red dot). GG—Garwood Glacier. Base map is light detection and ranging (LiDAR) topography slopeshade. LiDAR data serve as the basis for the plotted contours.

stratigraphic analysis and inferred glaciofluvial processes with this regional model of glacial activity during the Pleistocene and Holocene.

GARWOOD VALLEY SURFACE FEATURES

Garwood Valley contains numerous surface units similar to those mapped in Miers and Marshall Valleys (Clayton-Greene et al., 1988; Dagele, 1985); unique features include their size, spatial distribution, exposure, and stratigraphic continuity. Field mapping, light detection and ranging (LiDAR) topography (Schenk et al., 2004), and *Ikonos* satellite image data form the basis for a new surficial geologic mapping of Quaternary glaciofluvial units within lower Garwood Valley (Figs. 2 and 3).

This mapping shows that the lower end of Garwood Valley is dominated by the down-valley till unit, typically mapped as the Ross I drift (Stuiver et al., 1981) or the M3 drift unit (Richter, 2011). The surface of the till is composed of an angular

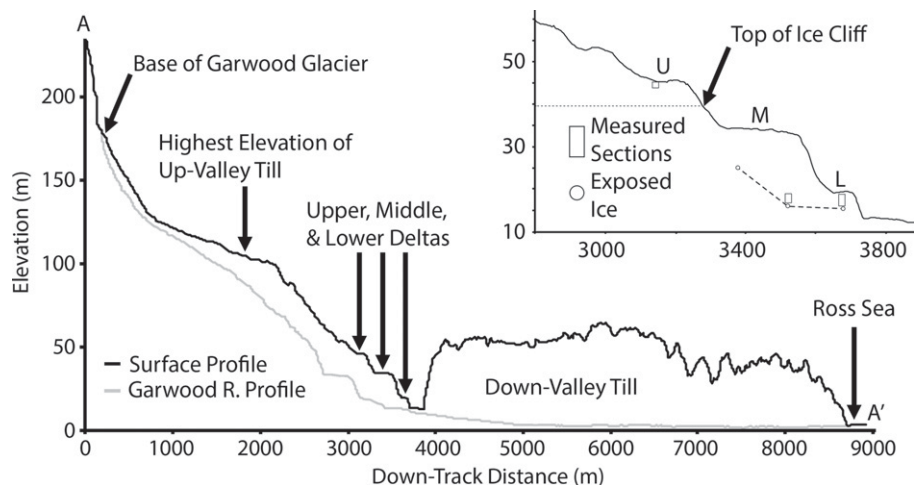


Figure 3. Topographic transects in Garwood Valley. Light line shows the main trunk of Garwood River. Dark line shows valley surface profile (dotted line in Fig. 2). Inset shows a higher-resolution view of the delta complex, with locations of mapped stratigraphic section and elevations of exposed ice. The dashed line interpolates the ice-sediment contact between outcrops. Topography was extracted from 4 m/pixel light detection and ranging (LiDAR) data (Schenk et al., 2004).

pebble-cobble-boulder desert pavement overlying unsorted silt and sand with sporadic larger clasts. Desert pavement cobbles are predominantly dark volcanics (dolerite and/or fine-grained phonolite) and orange metasediments, with sparse granite and sandstone boulders. Porphyritic anorthoclase phonolite (“kenyte”) is common in the down-valley till. Hyaloclastite breccias containing phonolitic glass are also present in the down-valley till. The lithic assemblage in the till is interpreted to indicate a dual source for till clasts that combines Ross Sea volcanic complex mafic rocks with granites, sediments, and metasediments derived from the Transantarctic Mountains south of Garwood Valley (Stuiver et al., 1981).

The down-valley till is universally underlain by massive glacier ice with a smooth, planar contact between the ice and the overlying sediments, suggesting that it is a supraglacial ablation till, rather than a subglacial till that has been exhumed. As noted by Pollard et al. (2002), the till is typically ~10–20 cm thick, although, in places, it thickens up to 1–2 m; however, all soil excavations conducted by the authors on the down-valley till between 2009 and 2012 have exposed buried ice beneath till. The down-valley till is extensively modified by thermokarst ponds (referred to as kettles by Pollard et al., 2002), resulting from melting of the underlying ice and evaporation of the meltwater. As a consequence of containing a massive ice core, the down-valley till unit has steep flanks and a generally convex-up surface profile (Fig. 3).

The up-valley till unit covers the valley floor between the down-valley till and the Garwood Glacier. The up-valley till shares many attributes with the down-valley till. The desert pavement at the top of the till is composed primarily of angular pebbles and cobbles, with boulders present less commonly than in the down-valley till. The underlying sand-silt matrix is much the same; however, it is generally slightly more oxi-

dized than the down-valley till. While all rock types present in the down-valley till are present in the up-valley till, “kenyte” is less common in the up-valley till, and it is not present in the northwesternmost third of the unit (the furthest up-valley). Where porphyritic anorthoclase phonolite (“kenyte”) is present in the up-valley till, it is typically fragmented. Hyaloclastite is extremely rare in the up-valley till, and, where present, it is strongly weathered. Although only locally exposed by Garwood River erosion and shallow soil excavations, the up-valley till is also underlain by massive ice, suggesting that it, too, is a supraglacial till. Thermokarst ponds are not present in the up-valley till, and it has a relatively uniform, down-valley surface slope (Fig. 3). Contacts between the valley walls, the up-valley till, and adjacent surface units are generally topographically smooth. The presence of two tills in Garwood Valley is consistent with observations in the McMurdo Dry Valleys of two or more till units associated with the Ross I drift (Denton and Marchant, 2000).

After the till units, the most notable surface feature in Garwood Valley is the large delta relict complex located in the center of the valley (Figs. 2 and 4). The three stepped deltas that form the complex are ~650 m in total length and ~280 m at their widest. The surfaces of the deltas step lower in the down-valley direction, from 45 m above sea level (a.s.l.) (upper delta), to 35 m a.s.l. (middle delta), to 20 m a.s.l. (lower delta). A small, isolated packet of till (interpreted as up-valley till) outcrops at the surface between the middle delta and the lower delta.

The deltas have a complex stratigraphy (see next section), but they are overwhelmingly composed of bedded, coarse, quartzofeldspathic sand. The surfaces of the deltas are topped with a desert pavement composed of rounded and subrounded pebbles that are predominantly representative of local metasediments, suggesting a source of deltaic sediments from within Gar-

wood Valley. Modern sand-wedge polygons dissect the upper several meters of the deltas. The delta complex is bounded by modern alluvium, which embays it on three sides and is in contact with the up-valley till to the northwest. The contact of the delta deposits with the up-valley till is sharp and is defined by a change in slope, lithology, grain size, and grain shape.

The Garwood River, which is fed by runoff from the Garwood and Joyce Glaciers, cuts through these units as it flows to the Ross Sea. Where the river cuts the up-valley till, the channel is tens of meters wide, >4 m deep, and steeply V-shaped. Observations of exposed ice in the channel walls (see “Other Ice-Sediment Relationships” section) and of river passage through undercut banks and/or tunnels through the up-valley till indicate that this portion of the river is affected by fluvial thermokarst formation in which relatively warm Garwood River water melts buried ice and undercuts the up-valley till, leading to surface subsidence.

Finally, in the vicinity of the relict deltas, the modern Garwood River and discharge from several snow-fed gullies on the valley walls form a surface unit of modern alluvium. Recent deposition is chiefly in broad flats adjacent to and downstream of the delta complex. Modern alluvium is predominantly quartzofeldspathic sands with millimeter-scale horizontal bedding; however, finer particles, including silts and clays, are deposited by some distributary streams.

GARWOOD VALLEY DELTA COMPLEX STRATIGRAPHY

The stratigraphy of the Garwood Valley delta complex has been recently exposed by lateral erosion of the Garwood River. Taking advantage of these recent and short-lived exposures (they are rapidly being covered by colluvial and eolian deposits), we documented the stratigraphy of each of the three deltas during the austral summers of 2009–2012, with particular attention to relationships between sedimentary units within the delta complex, and between the sedimentary units and underlying massive ice (Tables 1–3).

The upper delta is spatially extensive, but it has sparse exposure, owing to its topographic isolation from the Garwood River, which has laterally eroded into the middle and lower deltas (Fig. 4). As a result, the flanks of the upper delta are generally mantled in steep, dry talus. A small outcrop of the upper delta was measured on the northeastern edge of the unit, where it is partially eroded by a small gully.

The base of the upper delta outcrop consists of medium to coarse sand and pebbles interpreted as fluviodeltaic sediments. Above the sands, a dark silty layer grades into a light-toned silt-clay

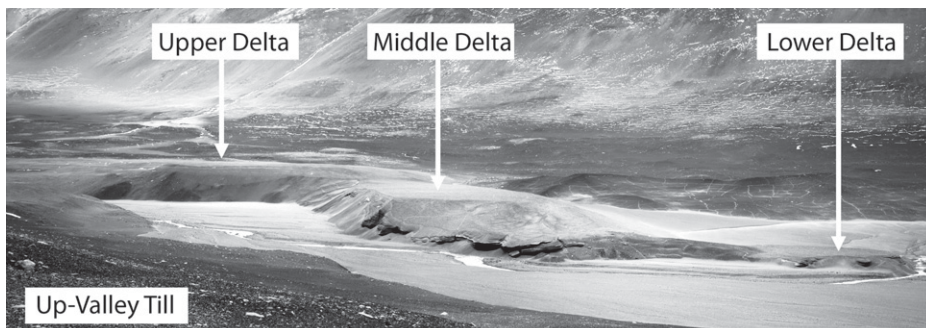


Figure 4. Ground view of the Garwood Valley delta complex. The deltas have a sharp, but topographically smooth contact with the up-valley till and are embayed by modern alluvial and fluvial sediments. The delta complex is ~650 m in total length and ~280 m at its widest.

TABLE 1. STRATIGRAPHIC DETAILS FOR THE UPPER DELTA

Unit/thickness	Upper delta unit description	Interpretation
G05 2 cm	Sandy gravel with surface pebble lag. Maximum clast size is 3–4 cm. Diverse lithologies are present, including quartzofeldspathic granites that are subrounded and coarse mafic volcanic clasts that are angular to subangular. Some mafics contain vesicles. The unit is uncemented and is variable in thickness from 1 to 5 cm, with a very irregular contact its base.	Desert pavement composed of winnowed fluviodeltaic bed load and eolian fines
G04 44 cm	Light-gray, clayey silt finely laminated at ~1 mm intervals. Thicker gray silt laminations are separated by silt partings. Unit is interbedded with thin semicontinuous lenses of dark-gray silt. The bedding of both silt layers is locally disrupted. Some beds are traceable continuously across the whole outcrop. The boundary between light and dark bands is irregular but generally traceable across the outcrop. Isolated pebbles up to 5 mm in diameter are present throughout the silt. The lower contact is irregular and is marked by a change in grain size from dark silt to light clay-silt.	Interbedded suspended load silt and clay with admixtures of darkaeolian silt, which underwent subsequent ice-related deformation
G03 12 cm	Poorly compacted, structureless dark-gray silt containing sparse, fine- to medium-grained sand. The sand is composed of mafic grains and micas, and it is well-sorted. Chips of the upper (G04) silt are present. The thickness of the unit varies between 6 and 15 cm and is continuous across the exposure, with an apparent dip of ~15° due east. The lower contact is sharp and planar, but it climbs at the east end, suggesting the former presence of a topographic depression.	Wind-emplaced silt
G06 18 cm	Medium to coarse sand beneath a 2-cm-thick ice-cemented gravel cap composed of subangular to subrounded clasts of diverse lithologies. The largest clasts in the cap are ~2 cm in diameter and consist of quartzofeldspathic metasediments and mafic volcanics. The gravel is generally light gray and loose where dry (ice-free). Coarse stringers of gravel are present in some portions of this unit. The gravel is poorly sorted, and subtle subhorizontal bedding is present, defined by grain-size variations, including interbedding of pebbly and sandy layers. The gravel coarsens upward toward the contact with the G03 silt. The bottom contact is not exposed; however, based on observations of inaccessible outcrops on the riverward side, the layer is likely several meters thick. The contact with the G03 silt is muddy, with silt infiltrating 1–5 cm into the gravel.	Fluviodeltaic bed load associated with the formation of upper delta topsets

unit along an irregular contact, interpreted to be eolian silts (lower, dark-toned) and cryoturbated fluvial and eolian silt-clay, respectively. Finally, the upper delta is capped by a desert pavement composed of winnowed fluviodeltaic bed load and eolian fines. Based on the stratigraphic observations (Fig. 5; Table 1), we interpret the upper delta outcrop to represent topset delta deposits interbedded with eolian sediments, and overlying fluvial gravels, crosscut by 1–2-cm-wide, modern sand-wedge thermal contraction crack polygons.

The middle delta has the largest exposed section of the three major Garwood deltas (Fig. 6; Table 2). It was extensively undercut by the Garwood River in 2009, resulting in the formation of steep faces of ice-cemented sediment that persisted through 2010. By the austral summer of 2011, avulsion of the Garwood River away from the delta, coupled with sand-wedge-mediated block failure, resulted in dry talus piles developing at the foot of the outcrop, limiting access.

The lowest unit in the middle delta is a crudely bedded gravely sand containing relict sand wedges that is interpreted as an intact supraglacial till. The till has a sharp, planar contact with underlying massive ice. The till is capped by finely laminated clay and silt, interpreted as low-energy lacustrine sediments. Above this, a sequence of coarse sands fines upward to a finely bedded clay and silt unit, interpreted as fluvial deposits transitioning back into lower-energy lacustrine deposits. These upper lacustrine beds transition into a mixed sand and pebble fluvial lacustrine unit, which grades into a complexly fractured and bedded gravelly sand-silt unit that is interpreted as glacial till transported and emplaced by the “lake ice conveyor” (see following discussion; Clayton-Greene and Hendy, 1987; Hall et al., 2000b). Above the lake-ice modified till, a final silt-clay lacustrine bed grades conformably into several meters of bedded sand and gravel that are interpreted as deltaic foresets.

We interpret the overall stratigraphy of the middle delta outcrop (Table 2) to indicate inundation of a supraglacial till (G21 and G23) due to damming of the Garwood River. Initial lake formation was low energy, resulting in preservation of near-surface till features (e.g., fossil sand wedges; Fig. 7), and deposition of lacustrine unit G20. Lacustrine deposition alternated with fluvial deposition as the lake grew, producing the G19 sands, the G18 silts, and the G17 transitional sands.

The “lake ice conveyor” is a mechanism whereby glacial drift is rafted on proglacial lake ice cover toward the center and distal edges of the ice-covered proglacial lake. The ice cover acts as a filter and transports fines through the ice, resulting in smoothly laminated, fine-grained,

reworked till overlying lacustrine sediments in the McMurdo Dry Valleys (Clayton-Greene and Hendy, 1987; Hall et al., 2000b). Activity of the lake ice conveyor (Clayton-Greene and Hendy, 1987; Hall et al., 2000b) to modify proximal glacial drift into the G15 and G16 units is inferred based on the enhanced sorting of these units (compared to unmodified drift/till in G21 and G23) and the presence of compressive fractures in G16 interpreted to indicate deformation of wet sediment. The onset of lake ice conveyor activity may have resulted from hydrological changes (expansion of the lake) or for glaciological reasons (re-advancement of the ice sheet plugging the valley mouth).

The lower delta is smaller than the middle delta, but it is also well exposed by recent Garwood River erosion (Fig. 8; Table 3). Abundant algal mats in the lower delta also provide multiple radiocarbon dates (see section on “Synthesis of Delta Complex Stratigraphy”).

The lower delta, like the middle delta, has a sandy-silty-cobbly gravel as the lowest exposed unit, which is interpreted as a glacial till modified by lake ice conveyor processes, based on the presence of fine-grained interbeds. Above the till, a silt-sand layer coarsens upward into a sandy gravel, which we interpret as lacustrine sands grading upward into a braided channel deposit. A cross-bedded sand-silt unit overlies the sandy gravel and is interpreted as a deltaic topset deposit. Above this, the lower delta is capped by a gravelly sand fluvial unit that has been dissected at the top to form a pebble-rich desert pavement.

The stratigraphy of the lower delta leads to a general interpretation that it formed after the middle delta, in a proglacial lake setting, as deltaic deposition advanced to lower portions of the lake in response to lake-level lowering caused by thermokarst downcutting of the ice plug and/or ice-sheet lowering. The emplacement of the lower delta represents the final phase of lacustrine deposition in Garwood Valley (outside of modern thermokarst ponds), as it is topographically lower than any other delta surface in the mapped section of the valley. Based on the absence of evaporite deposits associated with the lower delta, further downcutting of the ice plug subsequent to the formation of the lower delta is inferred to have resulted in the final draining of glacial lake Howard.

Do the upper and lower till units described in the middle delta correlate with surface units mapped in the “Garwood Valley Surface Features” section? We note that the till island preserved between the middle and the lower delta and the down-valley till (Fig. 9) shares a similar lithology and low degree of weathering with the down-valley till. Likewise, the down-valley till

TABLE 2. STRATIGRAPHIC DETAILS FOR THE MIDDLE DELTA

Unit/thickness	Middle delta unit description	Interpretation
G13 73 cm	Stratified sand and gravel. The unit is dominated by poorly to moderately sorted, pebble-based gravel layers separated by 5–10-cm-thick packages of plane-bedded silt-to-sand layers. Fine, <1-mm-thick, horizontally bedded, silt laminae internal to these sand-silt packages are present and commonly contain frozen algal mats (see "Synthesis of Delta Complex Stratigraphy" section for treatment of chronology). The gravel clasts are surrounded by angular and are a mixture of mafics, volcanics, and quartzofeldspathics with a maximum clast diameter of ~5 cm. The sand and gravel beds thicken and coarsen upward and to the west (up-valley). This unit continues upward to the top of the middle delta, ~12 m above; however, the steep slopes of the outcrop make it inaccessible. The lower contact of this unit is sharp and conformable.	Fluviolacustrine sediments forming deltaic foresets
G14 17 cm	2–4 cm of plane-bedded silt and clay overlain by ~15 cm of plane-bedded sand, silt, and clay. Silt-clay beds are tan to off-white and are present in horizontal laminae, <1 mm thick, that are separated by thin silt-sand laminae. These laminae are parallel and locally wavy. Continuous coarse-to-fine sand horizons are present in the sand-silt-clay package. The deposit is well sorted and fines upward. Small, ~45° conjugate fractures are present between the basal clay and the overlying sand-silt-clay. Algal mats are present along beds in this unit. Slightly iridescent secondary ice lenses are present in the basal silt-clay that locally disrupt the bedding (likely formed by modern frost heave). The lower contact is sharp and wavy with an amplitude of ~30 cm and a wavelength of ~2 m.	Lacustrine deposit (deltaic bottomset)
G15 25 cm	Poorly sorted cobbly, sandy gravel that fines upward to coarse sand. It is generally clast supported with silty-clay matrix throughout. Clasts are angular to subangular and are chiefly mafic volcanics with <1% quartzofeldspathics. Large clasts are <10 cm diameter, with one large mafic clast ~25 cm in diameter. Some clasts have thin, patchy, tan-colored surface coating (carbonate), similar to basal coatings on the rocks of the modern up-valley and down-valley till units. No obvious bedding is present, although there is some subtle stratification in the upper sand. The maximum thickness of the bed is 30 cm, with a typical thickness of ~25 cm. The unit's lower contact is sharp and irregular and is locally marked by ~1 cm of silt-clay filling interstices between gravel clasts.	Lake ice "conveyor" deposit (Clayton-Greene and Henty, 1987; Hall et al., 2000b)
G16 65 cm	Poorly indurated gravely sand and silt. It is matrix supported, with sparse <30-cm-diameter clasts that are round to subangular. The round clasts are mostly granitic and are rare compared to the angular mafic clasts. The largest clasts congregate near the top of the exposure. Some clasts have a thin, patchy, tan-colored carbonate coating similar to basal coatings on the rocks in G15. Discontinuous lenses of stratified silt, sand, and gravel are present, and are up to ~20 cm thick. The upper half of these lenses is siltier, while the lower half is sandier. The silt component is yellow. Notably, the entire exposure is strongly fractured, with imbricate cracks dipping 30°–45° to the east (down-valley). The lower contact is gradational over ~5 cm and generally horizontal with very slightly waviness.	Lake ice "conveyor" deposit, similar to G15, that underwent compaction during the loading of the unit by G15
G17 11 cm	Fine-to-medium sand that coarsens upward to a coarse-pebbly sand. Isolated subangular mafic pebbles up to 4 cm in diameter are present, as are thin, wavy silt and very fine sand laminae. The sand layers have local sorting following the silt beds, yielding a horizontally stratified appearance. Similar to the overlying G16 unit, 40°–50° cracks in this unit dip to the east (down-valley). The lower contact is gradational over 2 cm.	Transitional facies between fluviolacustrine deposits (see below) and conveyor-modified till
G18 12 cm	Parallel laminae of silt with very fine sand partings. The silt laminae are <2 mm thick, with most much thinner. Some interbedded sand, granules, and ~1-cm-diameter pebbles are present in the lower 2 cm of the unit. The upper 2 cm section of the unit has reworked silt aggregates ~1 cm diameter. Silt bedding is wavy, particularly near the base of the exposure, and appears to fill abundant ripple troughs at the base of the unit. Numerous ~45° fractures dip to the east (down-valley) but are less abundant than in G17. Segregation ice lenses up to 2 cm thick are abundantly present in the silt. The lower contact is gradational over 2 cm with interbedded silt and cross-bedded sand.	Lacustrine deposits
G19 39 cm	Medium to coarse sand that fines upward to fine sand. The sand is generally gray with diverse lithologies, although the bedding is defined largely by variation between mafic and quartzofeldspathic compositions. Local very fine sand and silt laminae are present filling ripple troughs. The lower portion of the unit has wavy/rippled laminae, which transition upward to planar, horizontal bedding. Toward the bottom of this unit, a band of pebbly, medium to coarse sand is present containing isolated 2–3-cm-diameter pebbles and rip-up clasts of the underlying silt beds. The unit is very indurated, and the lower contact is sharp and wavy to planar.	Fluvial deposit that modifies the underlying lacustrine material
G20 23 cm	Tan clay and silt with fine-to-medium, gray sand interbeds up to 2 cm thick. The sand interbeds are mainly in the lower 10 cm of the unit. Mud overlies and fills sand ripple structures. The upper 10 cm section of the unit is parallel-laminated silt and clay with fine sand partings. Laminae are ~3 mm thick. Segregation ice is common in the upper silt and is rare in the lower sand. Generally, the lower boundary of the unit is sharp and irregular; however, locally, up to 1 cm of silt infiltrates into the underlying unit.	Low-energy lacustrine sediments
G21 90 cm	Gravelly, silty sand. The unit is poorly sorted, and the gravel is matrix supported by yellow silty sand. Gravel clasts are angular and are composed of diverse lithologies: ~50% mafic volcanics, with common orange metasediments (these metasediments are largely absent in G15). Discontinuous pockets of volcanic clasts are present and are better sorted than the rest of the unit. Some bedded structure is present in the unit, similar to subtle bedding observed in exposures of the down-valley till and at the little ice cliff, which dips slightly to the west (up-valley). The unit is invaded by wide cracks filled with light-gray sand and silt. Some sand and silt fill is massive, while subvertical bedding and V-shaped pebble lineations are common in other cracks (Fig. 7).	Subaerial glacial till, largely unmodified by lacustrine conveyor process. Evidenced by the presence of intact sand wedges in the till. Relict sand wedges are only found in this unit in Garwood Valley. The increase in cobble and gravel abundance toward the top of the unit may indicate desert pavement formation by eolian removal of fines
G23 160 cm	Crudely bedded, gravely sand. The yellowish-gray sand is fine to coarse and is locally cross-bedded and planar laminated. The sands are interbedded with poorly sorted gravel lenses. The gravel is mostly mafic volcanics, but also includes rare metasedimentary clasts. The gravel cobbles are up to 15 cm in diameter, and the largest are subhorizontally oriented. With depth, the exposure becomes sandier and begins to contain segregation ice lenses. The lower contact is sharp, and slightly undulatory, and it is marked by a transition between sediment (G23) and underlying massive ice.	Lower portion of a till unit of similar composition to G21. Together, this unit, G23, and G21 constitute a lower till package, in contrast to the conveyor-modified till package comprised by G15 and G16

TABLE 3. STRATIGRAPHIC DETAILS FOR THE LOWER DELTA

Unit/thickness	Lower delta unit description	Interpretation
NA 2 cm	Gravel, cobbles, and pebbles. The gravel is subangular to subrounded and is composed of diverse lithologies including mafic volcanics and orange metasediments. The maximum clast size is 8–12 cm.	Desert pavement
G07 108 cm	Gravelly medium to coarse sand with pebble lamina. The pebbles are 2–3 cm in diameter and are subangular to subrounded. The sands are stratified with low-angle activation surfaces dipping ~10° toward the east (down-valley), highlighted by black sand lamina. The unit generally coarsens upward from sands and granules to pebbly sand. The lower boundary of the unit is sharp, with wavy parallel beds.	High-energy fluvial/braided channel deposit
G08 48 cm	Fine to medium-fine sand with interbedded silt. The unit has wavy, subparallel bedding defined by grain-size variations. The sand is light tan or buff and is composed mostly of quartz, with some feldspar. Medium to medium-coarse sand packages are interbedded within the fine to medium-fine sand and contain ~1-cm-thick lamina and cross-bedding. The unit is meltwater-saturated in some locations and discharges at the outcrop face. Rip-ups of algal mat fragments are common in this layer. The lower contact of this unit is sharp and subplanar and is defined by a thick black algal mat.	Fluviodeltaic deposits forming deltaic topsets
G09 48 cm	Sandy gravel. Prominent 5-cm-thick sand lenses climb to south in the gravel and pinch out. These sands overlie frozen gravel lenses. The gravel is matrix-supported in bedded coarse sand. The largest gravel clasts are 6–8 cm and are composed of diverse lithologies, including mafics, metamorphics, and quartzites. The gravels and the sand lenses are poorly sorted, with subtle stratification running parallel to unit boundaries. Pebble long axes parallel this subtle, subhorizontal bedding. The lower contact of this unit is gradational over 5 cm, climbs to south, and is locally deformed.	Braided channel deposit
G10 8 cm	Silty, fine, tan/gray sand. Strong, parallel bedding in this unit is defined by grain-size variations, with lamina up to 0.5 cm apart. Locally, the bedding is deformed by modern ice wedge and/or segregation ice growth. The lower contact of the silty sand is abrupt and is defined by changes in grain size.	Lacustrine sands
G11A/G11B 50 cm	Silty clay coarsening up to silt and very fine sand. The light-brown, silty clay is strongly bedded into parallel, <5 mm clay layers separated by silt and very fine sand beds <2 mm thick. White clay beds cap the unit with 2–3-mm-thick internal clay laminae, and similar clay beds are present at the base of the unit. Contacts within the silt beds and the bounding clays are gradational. In the lower clay, parallel bedding is defined by grain-size variations with sandy partings. The clay is friable along bedding planes and is well sorted. Pebbles and/or dropstones that deform the clay bedding are present in the clays. The deposit is substantially invaded by modern segregation ice lenses. The lower contact of the unit is sharp and climbs slightly to southeast (down-valley).	Low-energy lacustrine deposit that is an extension of the G10 lacustrine unit
G12 >40 cm	Sandy, cobbly gravel. The unit is clast supported with cobbles up to 15 cm diameter, fining upward to 1 cm pebble gravel. The clasts are mainly angular to subangular mafic volcanics, and many have carbonate rims similar to the rinds present on cobbles in the Garwood Valley till units. The matrix between clasts is medium to coarse sand, interbedded with silt and clay beds that are horizontally laminated and that are up to 5–10 cm thick. Many of these clay beds are extensively expanded by segregation ice. The lower contact of this unit is not exposed. The unit correlates with the upper till package from the middle delta outcrop (G15 and G16).	On the basis of the fine-grained interbeds between till-like layers, we interpret this unit to be glacial till reworked by the lake ice conveyor process

shows evidence of preserved shoreline terraces (see following), which suggest that the down-valley till may be the source of the lake ice conveyor deposits. Accordingly, we interpret the lower till package (G21 and G23) as the stratigraphic expression of the up-valley till, and the upper till package as the stratigraphic expression of the (modified) down-valley till.

Relationships between Delta Complex Sediments and Ice

Massive ice locally underlies the lowest till in the middle delta. This is most evident (although inaccessible) where erosion by the Garwood River undercut several meters from the deposit face in 2009, exposing bright white, massive ice beneath overhanging and ice-cemented till, lacustrine, and fluvial deposits (Figs. 10A and 10B). In addition, extant massive ice is present immediately beneath the middle delta sediments at several locations northwest of the outcrop described in Table 2, where it melts out during summer months, forming ephemeral gullies (Fig. 10C). Finally, the Garwood River undercuts the lower delta (Fig. 10D). A side channel to the Garwood River has tunneled into the bank, under the lower delta, and emerges from the bank several meters downstream. This observation suggests that beneath the G12 till/conveyor unit at the base of the lower delta deposit (correlated with the down-valley till; Table 3), there lies a submerged remnant of the lower till identified in the middle delta (G22 and G23) and/or massive ice that is currently undergoing removal by fluvial thermokarst erosion. The presence of massive glacier ice beneath the basal units in the middle and lower delta outcrops strongly suggests that the Garwood delta complex was emplaced directly above an ice-cored, supraglacial till unit that we infer correlates with the up-valley till.

Superficially, evidence of interactions between the paleolake and the ice-cored down-valley till in Garwood Valley is preserved in the form of flat-lying benches incised into the down-valley till. The benches are ~1–2 m wide and tens to hundreds of meters long. We interpret these benches as shoreline terraces carved into the down-valley till (e.g., Fig. 11, which shows a shoreline terrace just above the lower delta topographic level). In the Garwood Valley delta complex, we see evidence of lake ice conveyor deposits interbedded with fine-grained lake sediments, as well as lake sediments overlying supraglacial till (which, in turn, overlies massive ice). This relationship, in which basal glacier ice is preserved beneath an intact supraglacial till, and overlying lake sediments, may be unique in the McMurdo Dry Valleys.

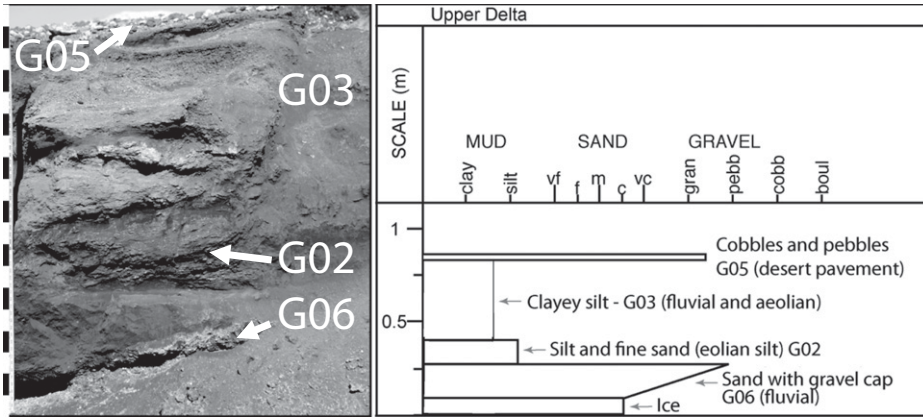


Figure 5. (Left) The upper delta outcrop. Scale bar at far left shows 5 cm vertical gradations. (Right) Stratigraphy of the upper delta. For sand, vf is very fine, f is fine, m is medium, c is coarse, and vc is very coarse. For gravel, gran indicated granules, pebb indicates pebbles, cobb indicates cobbles, and boul indicates boulders.

OTHER ICE-SEDIMENT RELATIONSHIPS

A surprising result of the stratigraphic analysis of the Garwood delta complex is that massive ice underlies the glacial till (inferred to be of Ross Sea ice sheet origin; see “Chronology” section) and lacustrine deposits. Is this pattern repeated elsewhere in the valley? Two locations

shed light on ice-sediment relationships: the Garwood Valley ice cliff and the little ice cliff.

The Garwood Valley ice cliff provides a vivid illustration of fluvial sediments overlying massive glacier ice and till (Fig. 12). Similar in appearance to the down-valley massive ice outcrop presented in Stuiver et al. (1981), the ice cliff adjacent to the delta complex is a location where a sedimentary unit abutting the up-valley till precipitously steps

down to the modern Garwood River braid plain, with a change in elevation of 10–15 m occurring over a horizontal distance of 2–3 m.

Although access to the sediment-ice contact at the top of the ice cliff is precluded by the dramatic relief, the stratigraphy of the interface was evaluated using fallen blocks containing the contact. The ice cliff material is largely composed of clean and variably bubbly glacial ice with low debris content (except for in places where bands of ice-cemented sands are present in horizontally bedded packages ~10–30 cm thick). Above the ice, there is a pebble- and cobble-rich unit supported by a brown silty sand matrix. The pebbles are largely angular mafic volcanics, are concentrated toward the top of the unit, and are sparsely distributed throughout. Above the cobbles, there are coarse sands and granules that are plane-bedded with varying degrees of dip and festoon cross-bedding. Sand packets are typically several centimeters thick and are traceable for several meters across the top of the ice cliff. The cobble-rich unit is in conformable contact with the ice, and it has a sharp, but undulating contact, typical of the contact between buried ice and overlying sediment in the down-valley till. The overlying sandy layer invades the underlying cobble-rich unit over a several-centimeter gradational contact. Upward, the sands give way to a pebble-based

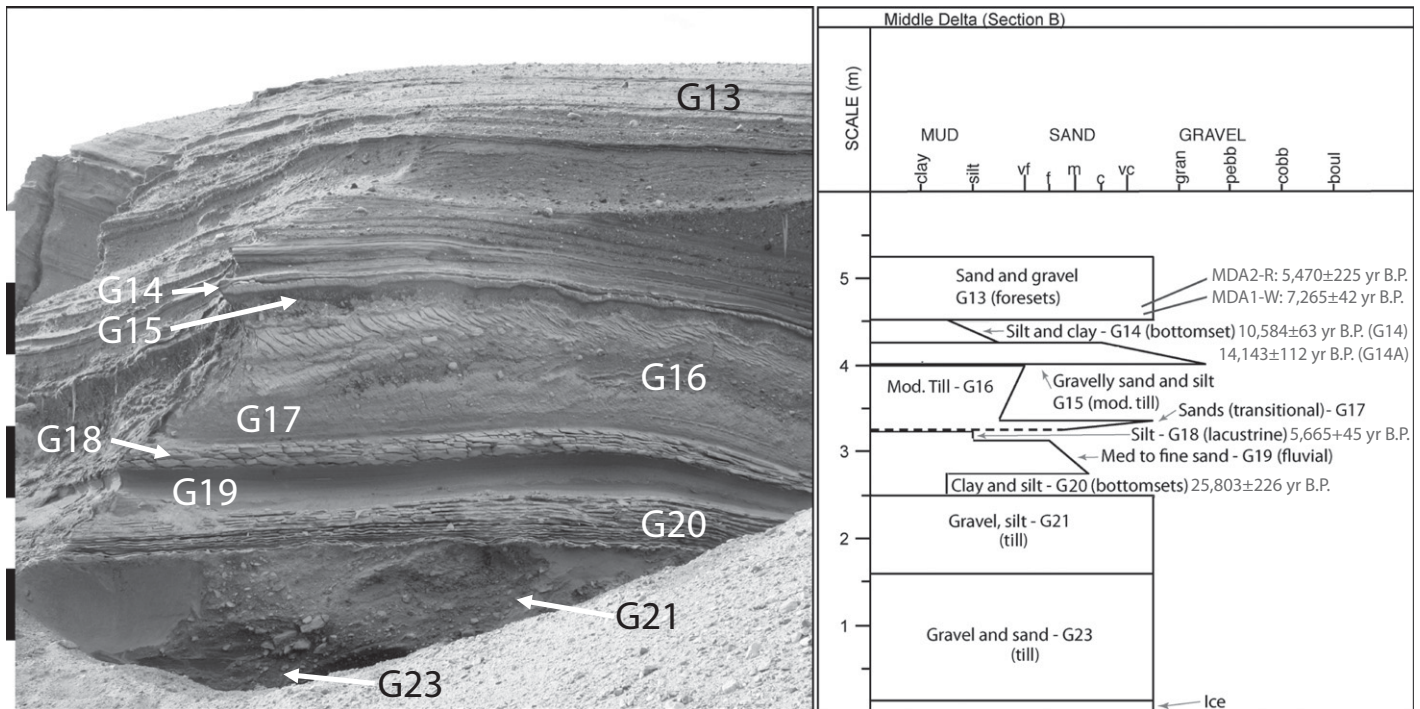
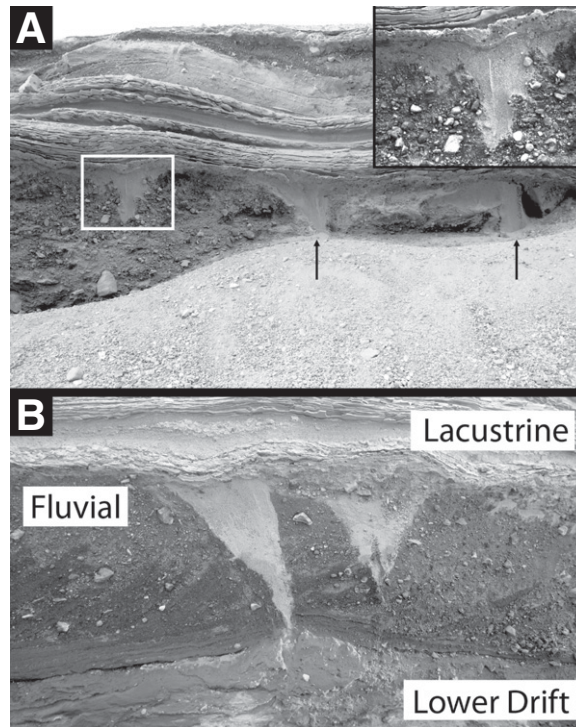


Figure 6. (Left) The middle delta outcrop. Scale bar at left shows 50 cm vertical gradations. (Right) Stratigraphy and age control for the middle delta. For sand, vf is very fine, f is fine, m is medium, c is coarse, and vc is very coarse. For gravel, gran indicated granules, pebb indicates pebbles, cobb indicates cobbles, and boul indicates boulders.

Figure 7. Relict sand wedges preserved in the lower till and in fluvial units contemporaneous with the lower till. (A) Sand wedge polygons (box and arrows) in the lower till. Inset shows a contrast-stretched image of the boxed sand wedge showing vertical laminations of sand, suggesting the sand wedge formed in situ and has been preserved intact. Sand wedges are ~1 m wide. (B) Sand wedges in a fluvial unit coeval with the lower till. Sand wedges are ~50 cm wide.



In contrast to this ice-sediment depositional environment, the little ice cliff, an outcrop located down-valley from the delta complex, provides insight into the relationship between the down-valley till and fluvial erosion (Fig. 13). The little ice cliff is an ~4-m-high exposure of massive ice embayed by the modern Garwood River braid plain, opposite the main body of the down-valley till. The ice contains stringers of sand, similar to those observed at the ice cliff, but which are generally thinner than 10 cm. A sharp upper contact marks the transition between the little ice cliff ice and overlying sediments. The sediment cover is dominated by yellow-tan sand and silt, containing sparse angular cobbles. The sands have subtle, subhorizontal bedding defined by varying degrees of sediment cohesion. The clast density increases toward the top of the sediment cover. Most clasts are mafic volcanics, and they range in size from pebbles to ~40 cm boulders. Many clasts have carbonate rind surfaces.

On the basis of its textural and compositional similarity with the down-valley till present across the modern Garwood River, we interpret the little ice cliff to be a portion of the down-valley till that was separated from the main body of the unit by Garwood River fluvial and thermal erosion (fluvial thermokarst). The presence of down-valley till upslope of the little ice cliff, grading into a topographically smooth contact with the valley-wall bedrock, suggests that there has not been significant fluvial and/or thermokarst erosion upslope of the little ice cliff. Rather, it suggests that the primary conduit for discharge for the modern Garwood River, and,

desert pavement at the top of the sediments above the ice cliff.

These ice-capping sediments form a small, but distinct and planar surface unit that abuts the up-valley till at a topographically smooth, but compositionally sharp contact. The sediments above the ice cliff form a relatively flat-lying surface that is ~3 m lower than the upper delta topmost surface. Taken together, we interpret

these relationships to indicate that the Garwood Valley ice cliff represents a location where stranded ice-sheet ice, overlain by till, was inundated and then buried by fluviodeltaic sediments associated with the delta complex. The ice cliff represents a simplified, marginal portion of the delta complex, and it illustrates the conformable contacts between buried ice, till, and fluviodeltaic sediments.

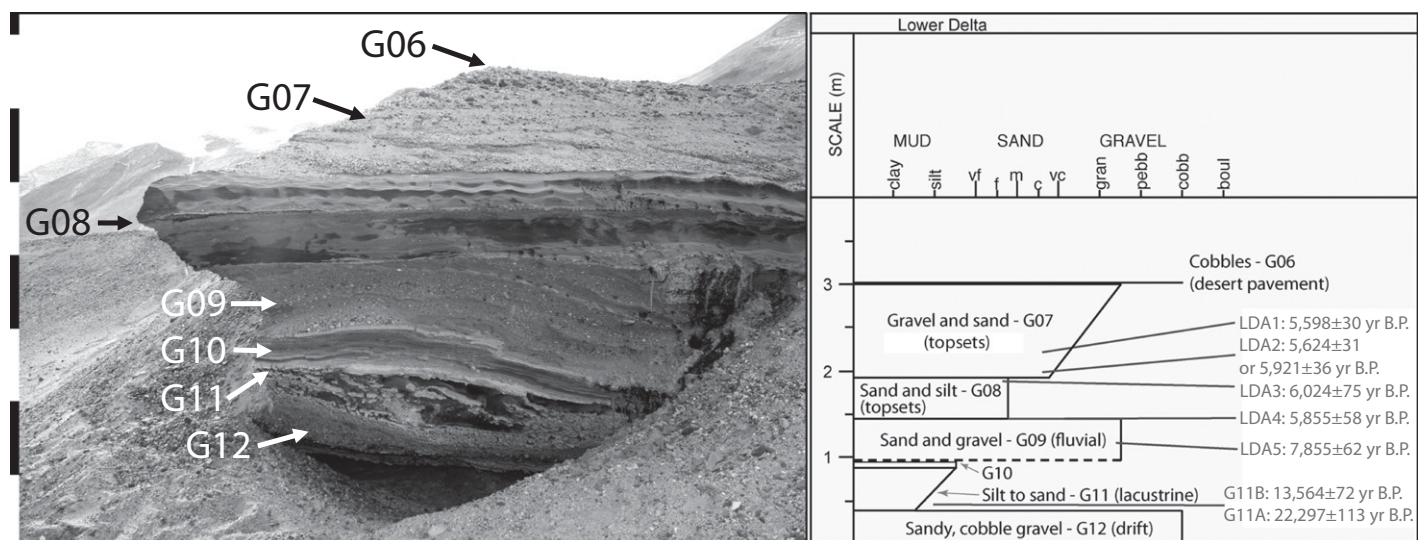


Figure 8. (Left) The lower delta outcrop. Scale bar at left shows 50 cm vertical gradations. (Right) Stratigraphy and age control for the lower delta. For sand, vf is very fine, f is fine, m is medium, c is coarse, and vc is very coarse. For gravel, gran indicated granules, pebb indicates pebbles, cobb indicates cobbles, and boul indicates boulders.

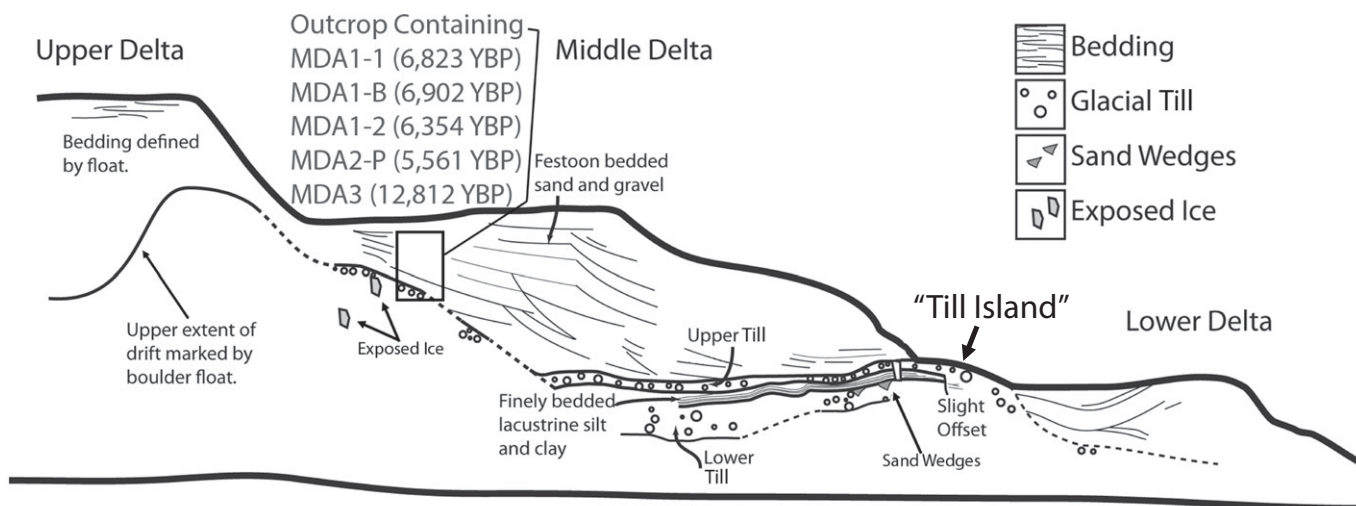


Figure 9. Composite sketch of the Garwood Valley delta complex based on field observations and annotated based on stratigraphic interpretations.

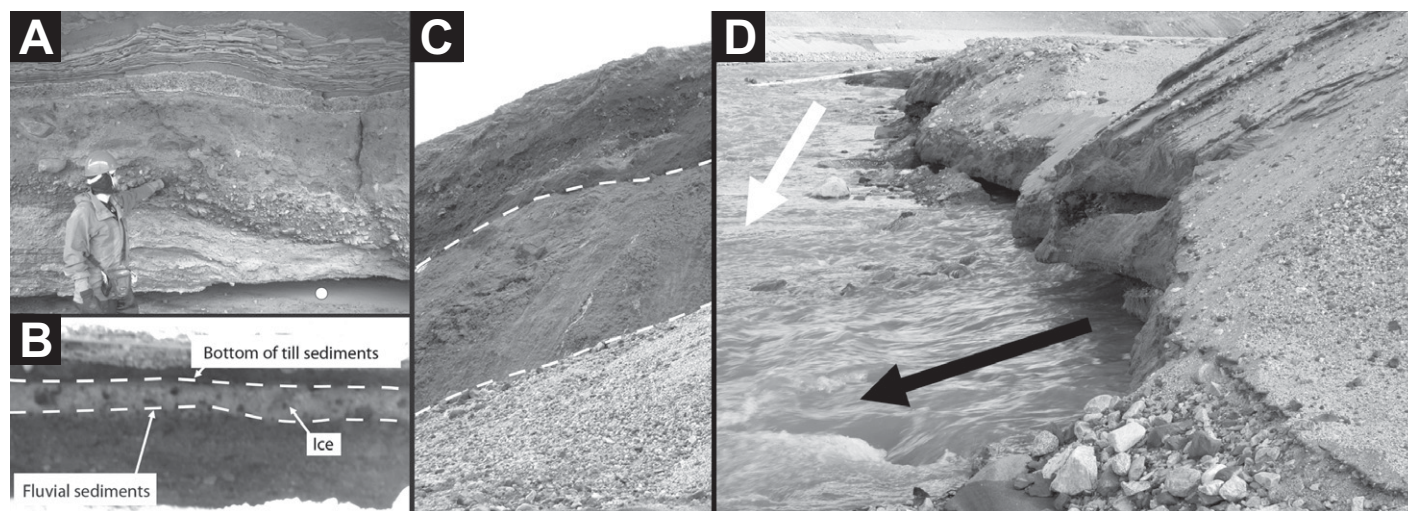
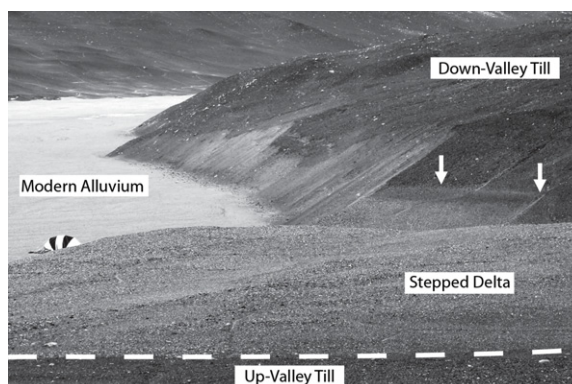


Figure 10. Contacts between sediment and ice. (A) A portion of the middle delta with the lower till indicated by pointing. White dot indicates the location from which part B was photographed. (B) View looking beneath the undercut middle delta. Till sediments are in an undulating contact with bright white ice. Exposed ice is bounded by dashed lines. Thickness of exposed ice is ~20 cm. (C) Exposed ice (bounded by dashed lines) beneath a portion of the middle delta. Height of exposed ice is ~1 m. (D) Undercutting of the lower delta by the modern Garwood River. Main channel flow direction is indicated by the white arrow. Flow from under the delta is indicated by the black arrow. Fluvial thermokarst erosion is common in Garwood Valley. Aluminum ladder in background (above white arrow) for scale. Ladder is ~4 m long.

Figure 11. A shoreline (arrows) incised in the down-valley till. The shoreline sits slightly above a terraced delta that is at nearly the same elevation as the lower delta, located across the modern Garwood River braid plain.



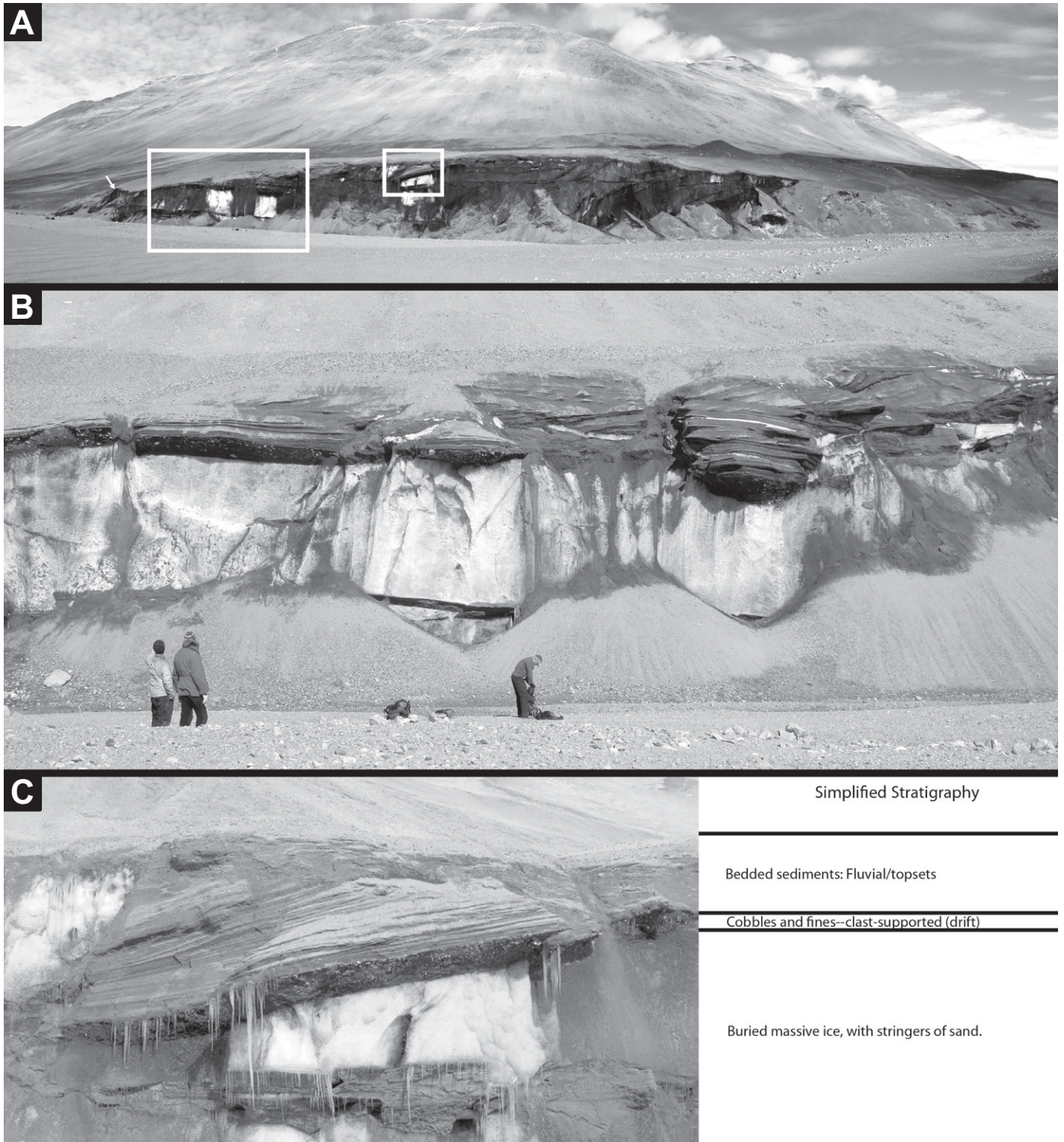


Figure 12. The Garwood Valley ice cliff. (A) Wide-angle view of the ice cliff, looking south from the Garwood River braid plain. White arrow indicates location of JLA10IC1. Large box indicates location of B; small box indicates location of C. (B) The ice cliff with people for scale. Bedded fluviodeltaic deposits above a coarse till layer are clearly visible. Talus cones formed from ice and sediment shed from above sit at the front of the ice cliff. (C) Close view and simplified stratigraphy of the ice cliff. Till sits atop massive buried ice; deltaic sediments sit atop the till.

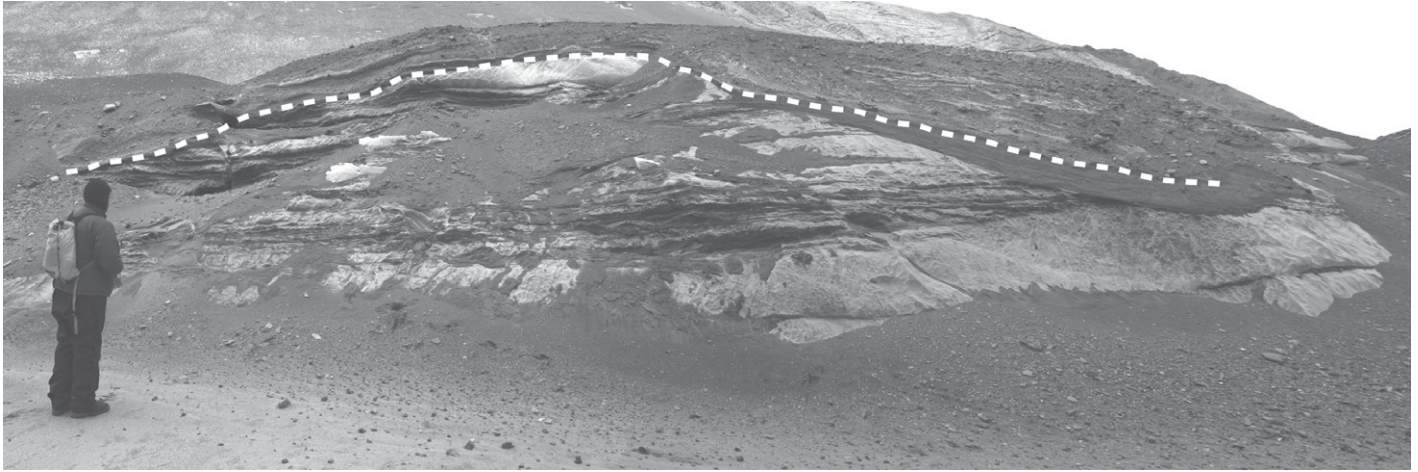


Figure 13. The little ice cliff. Massive ice sits below a coarsely bedded till deposit. Dashed line marks contact between massive ice with sand stringers and overlying till.

likely, for the paleo-Garwood River and/or Glacial Lake Howard, was through an eroded portion of the Ross Sea ice sheet ice dam that constitutes the down-valley till.

SYNTHESIS OF DELTA COMPLEX STRATIGRAPHY

Based on these stratigraphic observations and resulting inferences, we have correlated units among the upper, middle, and lower deltas to produce a composite picture of Garwood Valley delta complex stratigraphy (Fig. 9). Grain-size distribution summaries of units identified in this study are given in Figure 14. A schematic illustration of the glacial, hydrological, and geological processes that formed the Garwood Valley delta complex and surface units is presented in Figure 15.

At the base of the complex, a lower till unit overlies intact massive ice and was generated as a sublimation/melt-out lag deposit. At the surface, we map this unit as the up-valley till. The presence of a supraglacial till deposit in central Garwood Valley implies the emplacement of a large ice plug into the valley during LGM time. The best evidence for a Ross Sea ice sheet source for the ice dam is the similarity between the glacial till sediments in Garwood and the glacial till sediments mapped throughout the northern Dry Valleys (which, by virtue of geometry, cannot have been dammed by the Koettlitz Glacier; Stuiver et al., 1981; Denton et al., 1989; Hall and Denton, 2000). The sediments in the till units (mapped extensively in the past as the Ross I drift) are composed overwhelmingly of Ross Sea extrusive volcanics, rather than of Royal Society Range metasediments and intrusive volcanics. The Koettlitz Glacier is not a

strong candidate for the source of Ross Sea volcanic sediments; rather, we interpret the geology of the up-valley and down-valley tills to indicate that, during the LGM, the Ross Sea ice sheet was the dominant ice source for the Garwood Valley plug. Accordingly, in order for the ice dam to have formed, the Ross Sea ice sheet grounding line must have been located up to or north of the mouth of Garwood Valley.

A reentrant lobe of Ross Sea ice sheet ice, capped by sublimation lag deposits (the down-valley till), dammed the Garwood River, resulting in deposition of lacustrine deposits upstream of the dam. Depositional energy was sufficiently low to preserve till sedimentary structures, including sand wedges, as it flooded the lower/up-valley till. As the lake (Glacial Lake Howard) (Péwé, 1960) grew, calving of icebergs and down-valley till sediments from the glacier led to the deposition of glacial drift onto the lake ice, which was then rafted and deposited by the conveyor process (Clayton-Greene and Hendy, 1987; Hall et al., 2000b), forming the upper till in the middle delta.

Preservation of the deeply ice-cored down-valley till (including the presence of unconsolidated sedimentary features at the till surface such as the shoreline terrace) indicates that the ice overlain by the down-valley till was stranded at some point in Garwood Valley. Once cut off from the main Ross Sea ice sheet, it was too thin to flow rapidly and drain back out of the valley mouth and became dead ice.

Eventually, deltas formed in the ice-dammed lake in the Garwood Valley. First the upper delta formed. Lake level then dropped, which we interpret as a resulting from downcutting through the dead-ice plug, resulting in the middle delta forming in a lower and down-

valley position. A similar sequence followed to produce the lower delta. In order for the lake water to have drained, ice levels had to be lower outside of Garwood Valley. Because the mouth of Garwood Valley is at sea level, the Ross Sea basin into which the Garwood Valley drains has to have been free of grounded ice at the time of lake lowering, or else the lake would have continued to have been dammed by the high Ross Sea ice sheet ice. From the elevation of the deltas, approximate lake levels and areas (Fig. 16) can be estimated. Lake area dropped from $7.1 \times 10^5 \text{ m}^2$ during formation of the upper delta, to $2.9 \times 10^5 \text{ m}^2$, and, finally, to $1.3 \times 10^5 \text{ m}^2$ during formation of the lower delta (for comparison, total delta surface area is $\sim 1.1 \times 10^5 \text{ m}^2$).

The only unit in the complex that shows clear evidence for a period of subaerial modification is the lower till package, inferred on the basis of preserved sand wedges (which occur only in this unit in the delta complex and which form over $\sim 10^3$ yr time scales under persistent dry conditions). This, coupled with the absence of massive gypsum layers and large calcite crystals (common to Miers and Marshall Valley paleolake deposits) (Clayton-Greene et al., 1988; Dägel, 1985), suggests that the Garwood Valley paleolake (Glacial Lake Howard) never fully desiccated. This argues against major periods of evaporation (and attendant changes in lake chemistry) as the major driver of lake-level reduction, although climate-driven change to lake water budget and attendant lowering of lake level are possible explanations of the change in water level that resulted in the end of deposition on the upper delta and the formation of the middle delta. Rather, the evidence for extensive fluvial thermokarst erosion in the valley, coupled with the winding path of the Garwood

River through the remnant ice-cored portions of the down-valley till (Fig. 2), suggests that lake lowering most likely resulted from localized breaching of the ice dam and discharge to the Ross Sea. This delta expansion and lake-

level down-drop suggest that the Ross Ice Shelf grounding line had retreated south of Garwood Valley by the time that deposition ceased on the upper delta and transitioned to the middle delta, allowing paleolake water to drain.

CHRONOLOGY

Tying the relative chronology determined from the stratigraphic observations to absolute ages is key to determining the significance of the Garwood Valley sediment and ice deposits with respect to behavior of the Ross Sea ice sheet. During the course of the stratigraphic measurements and observations, we collected 21 samples of carbonaceous materials that were radiocarbon dated by accelerator mass spectrometry (Table 4). Most dated materials were samples of algal mats preserved within lacustrine and fluvial deposits. Also analyzed were six samples of lacustrine carbonate and a feather contained in glacial till. The chronologic information provided by these results is presented as both radiocarbon years (^{14}C yr B.P.) and as calendar years (cal. yr B.P. or ka, depending on precision) based on the Fairbanks et al. (2005) and INTCAL (Stuiver and Reimer, 1993; Reimer et al., 2009) radiocarbon calibration curves. These dates build upon previous radiocarbon dating of materials collected near the mouth of Garwood Valley (Denton and Marchant, 2000;

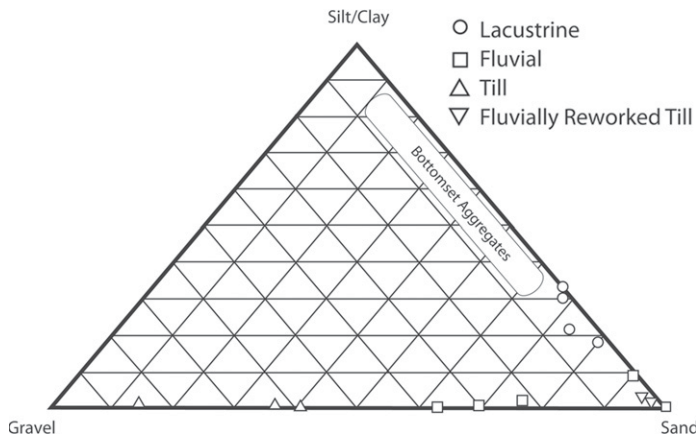
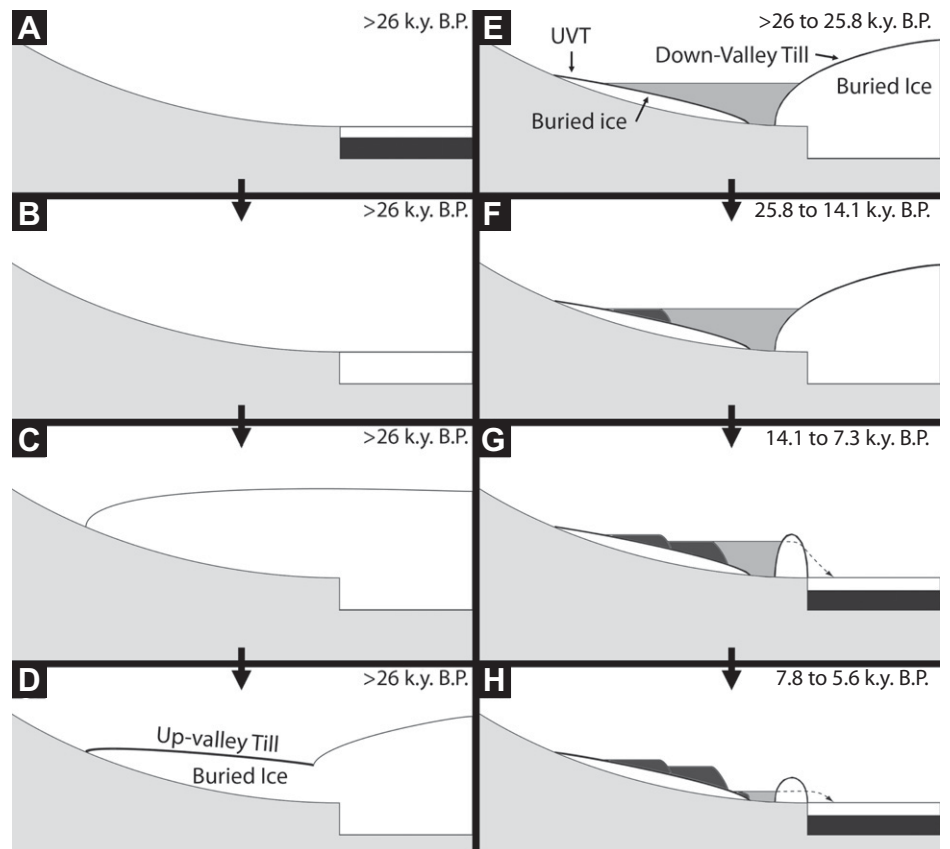


Figure 14. Ternary plot of Garwood Valley delta complex sediment sizes. Mixing ratios were calculated by mass. Sedimentary groups (e.g., till, fluvial sediments, etc.) broadly agree with grain-size distributions in Dagal (1985).

Figure 15. Conceptual diagram showing inferred evolution of the Garwood Valley paleolake and deltas. Dates are derived from ages in Table 4. (A) Garwood Valley during interglacial time. The Ross Ice Shelf (white) sits offshore, floating on the Ross Sea (black). (B) Expansion of the East and West Antarctic Ice Sheets during the Pleistocene thickens the Ross Ice Shelf, grounding it to form the Ross Sea ice sheet (white). (C) Continued growth of the Ross Sea ice sheet thickens the ice sufficiently to flow up-valley from the coast and into Garwood Valley, transporting the up-valley till with it (bold). (D) A period of ice-sheet stability allows ice in the upper reaches of the valley to sublimate and deflate slightly, while a resurgence of ice expands into the mouth of the valley, transporting the down-valley till atop it (bold). Up-valley till formation occurred at least 25.8 k.y. B.P., because it underlies the oldest dated carbonate beds, and the down-valley till is at least as old as 14.1 k.y. B.P. because reworked sediment from it is present in the middle delta. (E) The ice dam in the mouth of Garwood Valley blocks flow of the paleo-Garwood River forming a proglacial lake that superposes the up-valley till (UVT) and buried ice. (F) The upper delta forms in the ice-dammed lake. (G) Retreat of the Ross Ice Shelf grounding line south of Garwood Valley strands a portion of the ice dam in the valley. Thermokarst erosion of the ice dam (dashed line) results in lowering of lake level and deposition of the middle delta. (H) Continued ablation of the ice dam results in lowering of lake level and deposition of the lower delta.



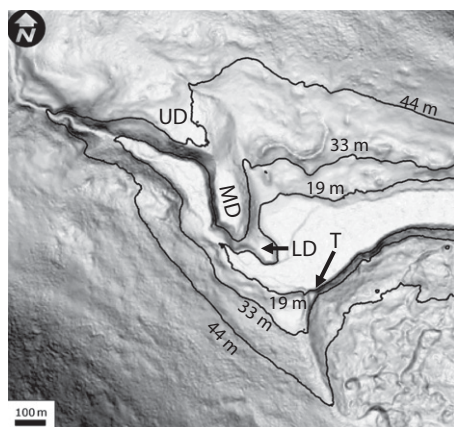


Figure 16. Approximate lake levels based on delta complex surface levels. Each black contour traces the delta top surface along the modern Garwood Valley topography, based on airborne light detection and ranging (LiDAR) measurements. Base map is slopeshade (light tone—low slope, dark—high slope) derived from the LiDAR. UD—upper delta, MD—middle delta, LD—lower delta, and T—the location of the shoreline terrace shown in Figure 11.

Stuiver et al., 1981) and directly address the hypothesis of Hendy (2000) that the Garwood Valley lake deposits are Holocene-aged.

Two major challenges exist for interpreting radiocarbon age data in the McMurdo Dry Valleys: (1) determining whether samples from perennially ice-covered lakes are from shallow-water environments that are in regular exchange with atmospheric CO₂ through seasonal moats

and surface water, or if they are from deep-water deposits that are cut off from atmospheric CO₂ due to strong density stratification (and would thus, appear older—the “residence effect”) (Doran et al., 1999; Hall and Henderson, 2001; Hendy and Hall, 2006); and (2) determining the correspondence between algal mat ages and lacustrine carbonate ages—do algal mats show evidence of incorporation of inheritance of old carbon from glacial or geological sources (the “inheritance effect”)?

Do Garwood Valley radiocarbon samples represent shallow-water or deep-water deposits? All of the algal mat samples derive from sedimentary units that are interpreted as foreset deposits (Tables 1–3). These deposits are interpreted to have formed in shallow lake water as the delta advanced, and are therefore likely to have been well ventilated. The sediment was transported by the paleo-Garwood River, which was also likely to have been in ready contact with the atmosphere. Deltaic bottomset beds bearing carbonates may have formed in deeper-water environments than the algal mats, however, because the paleo-Garwood River was the primary source for water entering the lake (see Geochemistry section), it is likely that the carbonate source waters were also well exchanged prior to carbonate formation. These factors suggest that residence effects are small in Garwood Valley radiocarbon dates, based on the Doran et al. (1994) and Hendy and Hall (2006) models of stream and lake moat mixing.

Do Garwood Valley algal mats show evidence of inheritance of old carbon? Three lines of evidence lead us to conclude that while old carbon may have been incorporated into the algal mats

sampled in Garwood Valley (e.g., from melt-water interactions with carbonate bedrock or old ice-sheet carbon), it does not significantly affect the derived radiocarbon ages. First, the presence of both highly depleted ¹³C values for the algal mats (–24‰ to –30‰) and enriched values (–5‰ to –10‰) (Table 4) suggests that some algal mats have incorporated geological carbon (enriched in heavy ¹³C), or that they may have formed without geological enrichment in the paleolake moat, where rapid CO₂ uptake associated with short growing seasons could have reduced fractionation and increased δ¹³C values to the –10‰ to +1‰ range (Brenda Hall, 2012, personal commun.). Regardless if the enriched algal mats are evidence of incorporation of old carbon, the position of the ¹³C-enriched samples stratigraphically above the unenriched samples, coupled with younger ages for the ¹³C-enriched samples compared to the unenriched samples, suggests that the effect of geological carbon input into the algal mats is small if present. Second, the radiocarbon age of a modern algal mat collected in a Garwood Valley thermokarst pond that is fed exclusively by melt of underlying Ross Sea ice sheet ice in the down-valley till unit is postbomb, indicating that there is little carbon inheritance into algal mats growing in ponds derived from melting of this portion of the Ross Sea ice sheet in Garwood Valley. In the absence of evidence for significant age offsets from old carbon reservoirs derived from bedrock or old ice, we adopt the radiocarbon ages derived from the algal mats at face value and calibrate them directly to calendar years.

In addition, ambiguity exists in the interpretation of radiocarbon ages obtained from lacustrine

TABLE 4. SUMMARY OF ALGAL MAT AND CARBONATE AGES DETERMINED BY AMS RADIOCARBON DATING

Sample	Type	Setting	Age (¹⁴ C yr B.P.)	δ ¹³ C (‰)	Age (cal. yr B.P.) (F)	Age (cal. yr B.P.) (F)	Age (cal. yr B.P.) (I)
JLA10ICD1	Algal mat	Modern pond	Postbomb	Postbomb	Postbomb	Postbomb	Postbomb
JLA10LDA1	Algal mat	Lower delta	4861 ± 41	–8.4	5598 ± 30	5606 ± 20	5606 ± 20
JLA10LDA2-1	Algal mat	Lower delta	4899 ± 40	–7.3	5624 ± 31	5626 ± 28	5626 ± 28
JLA10LDA2-2	Algal mat	Lower delta	5171 ± 42	–9.4	5921 ± 36	5927 ± 23	5927 ± 23
JLA10LDA3	Algal mat	Lower delta	5269 ± 49	–5.6	6024 ± 75	6098 ± 21	6098 ± 21
JLA10LDA4	Algal mat	Lower delta	5098 ± 40	–5.7	5855 ± 58	5791 ± 35	5791 ± 35
JLA10LDA5	Algal mat	Lower delta	7020 ± 54	–24.5	7855 ± 62	7852 ± 30	7852 ± 30
G11B	Carbonate	Lower Delta	11,702 ± 61	2.4	13,564 ± 72	13,544 ± 97	13,544 ± 97
G11A	Carbonate	Lower Delta	18,690 ± 110	3	22,297 ± 113	22,358 ± 75	22,358 ± 75
JLA10IC1	Algal mat	Ice cliff	6331 ± 58	–29.8	7259 ± 58	7277 ± 42	7277 ± 42
JLA10MDA2-R	Algal mat	Middle delta	4750 ± 190	–26.2	5470 ± 225	5502 ± 218	5502 ± 218
JLA10MDA1-1	Algal mat	Middle delta	5992 ± 42	–29.7	6823 ± 58	6836 ± 53	6836 ± 53
JLA10MDA1-W	Algal mat	Middle delta	6338 ± 44	–27.7	7265 ± 42	7282 ± 38	7282 ± 38
JLA10MDA1-B	Algal mat	Middle delta	6052 ± 43	–29.7	6902 ± 57	6904 ± 55	6904 ± 55
JLA10MDA1-2	Algal mat	Middle delta	5577 ± 63	–24.8	6354 ± 59	6356 ± 52	6356 ± 52
JLA10MDA2-P	Feather	Middle delta	4810 ± 42	–24.8	5561 ± 47	5508 ± 27	5508 ± 27
G14	Carbonate	Middle delta	9367 ± 51	3.8	10,584 ± 63	10,564 ± 45	10,564 ± 45
G14A	Carbonate	Middle delta	12,326 ± 63	3.3	14,143 ± 112	14,168 ± 104	14,168 ± 104
G18	Carbonate	Middle delta	4947 ± 42	–1.4	5665 ± 45	5681 ± 38	5681 ± 38
JLA10MDA3	Algal mat	Middle delta	10,920 ± 180	–7.5	12,812 ± 152	12,802 ± 166	12,802 ± 166
G20	Carbonate	Middle delta	21,480 ± 140	1.3	25,803 ± 226	25,722 ± 260	25,722 ± 260

Note: Ages are reported in both ¹⁴C yr and calendar years using the Fairbanks et al. (2005) calibration curve (F) and the INTCAL calibration curve (I) (Stuiver and Reimer, 1993; Reimer et al., 2009). AMS—accelerator mass spectrometry; cal.—calendar. AMS—accelerator mass spectrometry.

carbonates formed in ice-covered lakes (typical of modern Antarctica), in which exchange with atmospheric ^{14}C is limited by seasonal processes. Clayton-Greene et al. (1988) reported a maximum offset of 800 yr between radiocarbon dates of Miers Valley lacustrine carbonates and U/Th dating of the same carbonates. To within 1000 yr precision, then, radiocarbon dates of lacustrine carbonates may be considered an acceptable proxy for U-series dating.

In light of these considerations, what does radiocarbon dating of the Garwood Valley delta complex indicate about the timing of lake and delta formation? Dates for lacustrine bottomset material span from the latest Pleistocene into the Holocene, while ages of algal mats growing in the Garwood Valley delta environments are, with two possible exceptions, Holocene in age (Table 4). The sequence suggests that Glacial Lake Howard originated during ice damming of Garwood Valley at ca. 26 ka (ca. 21,000 ^{14}C yr B.P.). The absence of evaporates or other evidence for desiccation suggests that the lake persisted, with its level incrementally dropping until its demise sometime after 5.5 ka (ca. 4900 ^{14}C yr B.P.). The lower till, inferred to represent the more extensive up-valley glacial drift, apparently predates the 26 ka inception of the lake, and was subject to subaerial exposure prior to lacustrine inundation. The upper till, inferred to represent sediments derived from the younger, less-weathered, down-valley till that were reworked by the lake ice conveyor process, may be as young as 13–14 ka (ca. 11,000–12,000 ^{14}C yr B.P.) (Figs. 6 and 17).

What does the chronology indicate about the advance and retreat of the Ross Sea ice sheet grounding line? Damming of the paleo-Garwood River to produce the oldest dated carbonate beds requires the presence of an ice plug, which implies passage of the Ross Sea ice sheet grounding line north of Garwood Valley by 25.8 ± 0.2 k.y. B.P. (Table 4). This date is similar to other McMurdo Dry Valleys-derived grounding line passage estimates, ranging from ca. 23.5 k.y. B.P. in Taylor Valley (north of Garwood Valley) (Hall and Denton, 2000) to ca. 27.6 k.y. B.P. in Miers Valley (south of Garwood Valley) (Clayton-Greene et al., 1988). While the upper delta could have formed in an ice-sheet-dammed lake, with the grounding line still north of Garwood Valley, thinning of the Ross Sea ice sheet is required for partial drainage of Glacial Lake Howard, lake lowering, and the resulting growth of the middle delta. Algal mat ages from deltaic foresets in the middle delta span ca. 5470 to 7265 cal. yr B.P. (4750–6338 ^{14}C yr B.P.), indicating that incision of the ice dam began by ca. 7.3 ka (ca. 6300 ^{14}C yr B.P.). This result is consistent with an algal mat dated at 7259 ± 58

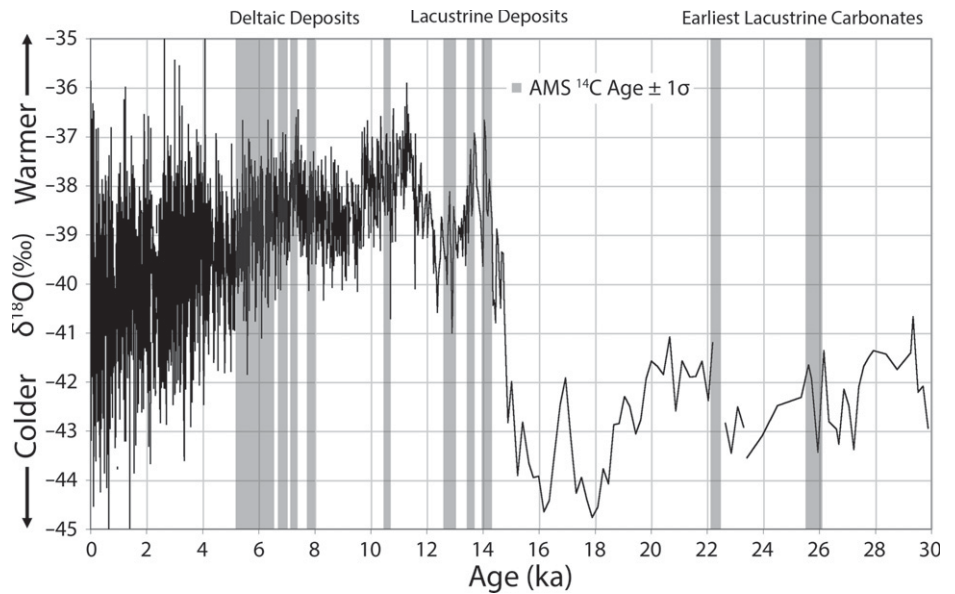


Figure 17. Plot showing the distribution of accelerator mass spectrometry (AMS) ^{14}C radiocarbon dates for the Garwood Valley delta complex plotted against the Taylor Dome $\delta^{18}\text{O}$ ice-core record (Steig et al., 2000). AMS radiocarbon ages were corrected to calendar years using calibration from Fairbanks et al. (2005). Width of individual carbon date bars reflects $\pm 1\sigma$ age error.

cal. yr B.P. (6331 ^{14}C yr B.P.) from the ice-cliff deltaic sediments, which sits at an intermediate elevation between the upper and middle deltas. Continued incision soon after formation of the middle delta is suggested by the very similar ages for the lower delta, which range from 7855 to 5598 cal. yr B.P. (7020–4861 ^{14}C yr B.P.), indicating that the Ross Sea ice sheet grounding line had moved south of Garwood Valley no later than 5.5 ka (ca. 4900 ^{14}C yr B.P.).

Interestingly, algal mat ages from the lower delta, which is stratigraphically younger than the middle delta (Figs. 8 and 9), span ca. 5598–7855 cal. yr B.P. (4861–7020 ^{14}C yr B.P.). In cases, these dates are older than middle delta algal mat dates. The relatively enriched ^{13}C content of most of the lower delta algal mat samples raises the possibility that inherited (old) carbon is present in lower delta algae, thereby resulting in slightly older radiocarbon ages for the stratigraphically younger deposits. Alternatively, the draping of the lower delta on the middle delta may have reworked older middle delta algal material and redeposited/incorporated it into lower delta algal mats, resulting in anomalously old ages for the lower delta mats.

These results are consistent with previous estimates of Ross Sea ice sheet grounding line recession past Garwood Valley ca. 4750–6338 ^{14}C yr B.P. (Conway et al., 1999; Denton et al., 1989; Denton and Marchant, 2000; Stuiver et al., 1981; Hall et al., 2004). The chronology

of lake-level drop derived from this study—initial lake-level decline at ca. 7.3 ka and lake demise by ca. 5.5 ka—is consistent with chronologies developed from dating of algal mats at the mouth of Garwood Valley. Stuiver et al. (1981) concluded that the Ross Sea ice sheet grounding line was south of Garwood Valley by 6580 ± 50 ^{14}C yr B.P. (equivalent to ca. cal. 7500 yr B.P.) and noted that ice-sheet level was at least below 25 m a.s.l. in Garwood Valley by 6190 ± 80 ^{14}C yr B.P. (5129 ± 96 cal. yr B.P.), and they argue that this date is compatible with, but is not direct evidence of, grounding line retreat.

Although it appears that downcutting through the wasting Ross Sea ice sheet and its remnants in lower Garwood Valley created the sequence of delta deposits and surfaces, what does the stratigraphy indicate about the initial growth of Glacial Lake Howard at ca. 26 ka and the subsequent transition from quiescent lacustrine deposition (carbonates and fine-grained silts) to high-energy deltaic deposition? The radiocarbon dates from our study (Table 4) are replotted over the Taylor Dome $\delta^{18}\text{O}$ record in Figure 17. This plot shows that the initial formation of Glacial Lake Howard occurred definitively during the Pleistocene, near the height of the LGM at ca. 26 ka.

Colder, drier conditions are thought to have persisted in the McMurdo Dry Valleys during the LGM, resulting in reduced glacier runoff (Doran et al., 1994). This was also the period

avored for the highstand of Glacial Lake Washburn in Taylor Valley (Hall and Denton, 2000). A possible resolution to this apparent paradox (proglacial lake development during cold, low-precipitation conditions) is that modern runoff in the McMurdo Dry Valleys is primarily driven by solid-state greenhouse effects within glaciers, rather than by sensible heat exchange (Hoffman et al., 2008; Hall et al., 2010). Accordingly, it is likely that the paleo-Garwood River remained at least partially active, even during extremely cold periods, driven by insolation-dominated melting. The formation of an ice dam in Garwood Valley during a low-discharge phase for the paleo-Garwood River is consistent with the initial formation of only fine-grained deposits over the ice and till at the base of the delta complex.

The next youngest radiocarbon dates from the delta complex (including carbonates and an algal mat) correspond with isotope maxima at the close of the glacial period. These samples span ca. 12.5–14 ka, which may correspond to local warming excursions in the McMurdo Dry Valleys associated with the positive $\delta^{18}\text{O}$ anomaly within the Antarctic Cold Reversal (ca. 12.8–14.5 ka) that produced increased runoff and changes to the paleolake depositional environment (Doran et al., 2008). Finally, the large cluster of algal mat ages from the mid-Holocene span a complex period of $\delta^{18}\text{O}$ variability in the Ross Sea sector. These deltaic depositional periods may have been associated with peak runoff and sediment transport years, or they may reflect more complex feedbacks among temperature, precipitation, and discharge in Antarctic seasonal rivers.

In summary, the radiocarbon dates from the Garwood delta complex broadly agree with previous interpretations of Ross Sea ice sheet grounding line retreat at the close of the LGM. The detailed chronostratigraphy of the delta complex suggests the persistence of an ice-dammed lake in Garwood Valley from pre-LGM through Holocene time. Rather than being a product of a single damming, filling, and draining sequence, the delta complex suggests a multi-stage history of lake filling, with transitions between fluvial, lacustrine, and glaciolacustrine processes operating in Garwood Valley over an ~20,000 yr period.

GEOCHEMISTRY

What does the composition of Garwood Valley ice and sediment indicate about its relationship with Ross Sea ice sheet ice and LGM-age sediments located elsewhere in Garwood Valley and in neighboring valleys? How representative is Garwood Valley of glaciofluvial processes in the southern McMurdo Dry Valleys? In this

section, we evaluate the chemical and isotopic compositions of Garwood Valley sediments and ice, relative to previous analyses of Garwood Valley deposits, and we compare them to samples from neighboring valleys.

First, in order to evaluate the continuity of buried ice composition in Garwood Valley, ice samples collected in 2009–2010 were analyzed for major ion composition and for $\delta^{18}\text{O}$ and δD (Fig. 18; Tables 5 and 6). Major ion concentrations were determined by ion chromatography as described in Welch et al. (2010), resulting in a total analytical error of <4%. Stable O and H isotopes were measured using a Picarro

WS-CRDS Analyzer for Isotopic Water, Model L1102-i. Samples analyzed for stable isotope ratios were splits from the major ion ice samples that were separated prior to ion chromatography (IC) analysis.

Comparisons of the major ion compositions and stable isotopes of Garwood Valley ice indicate broad similarities and intriguing differences between the Pollard et al. (2002) samples and the ice cliff/delta complex samples. Single-ended analysis of variance (ANOVA) analyses of the major ion data presented in Table 5 indicate no statistically significant ($P < 0.05$) differences between the buried ice at the mouth

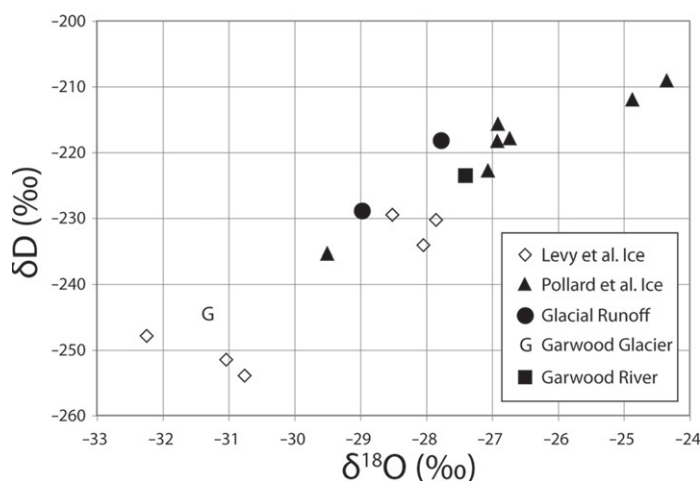


Figure 18. Plot of δD vs. $\delta^{18}\text{O}$ for ice and water collected in Garwood Valley. “Levy et al. Ice”—samples collected from the ice cliff and from beneath the delta complex. “Pollard et al. Ice”—values reported by Pollard et al. (2002). Glacial Runoff—water collected downstream of the Garwood Glacier. Garwood River—modern Garwood River water collected upstream of the ice cliff.

TABLE 5. MAJOR ION VALUES FOR ICE SAMPLES COLLECTED AT THE GARWOOD VALLEY ICE CLIFF AND FROM BENEATH THE DELTA COMPLEX (JLI SAMPLES), AND VALUES REPORTED IN POLLARD ET AL. (2002) (GMI SAMPLES)

Sample	F (mg/L)	Cl (mg/L)	SO ₄ (mg/L)	Na (mg/L)	K (mg/L)	Mg (mg/L)	Ca (mg/L)
JLI09G1	0.12	7.50	5.50	7.72	1.25	1.17	5.25
JLI09G2	0.19	3.97	5.38	10.92	2.12	0.88	6.08
JLI09G3	0.23	5.51	12.37	14.25	2.92	4.39	3.34
JLI09G4	0.05	2.88	0.33	2.50	0.68	0.52	3.62
JLI09G5		1.89	0.28	1.04	0.44	0.50	1.56
JLI09G6	0.09	4.76	4.94	7.70	2.04	1.04	11.97
JLI09G7	0.11	19.96	7.40	16.58	0.54	0.57	0.77
GMI42	0.08	10.90	2.41	12.90	1.81	0.73	2.10
GMI100	0.37	21.40	1.83	14.00	0.99	0.53	1.01
GMI200		122.00	4.28	67.90	2.25	6.84	2.81
GMI300		1.62	5.33	85.40	3.10	9.43	4.59
GMI400	0.10	30.60	1.69	18.30	0.79	1.21	1.05
GMI600	0.27	1.59	0.43	1.40	0.65	0.14	0.63
GMI800	0.09	0.47	0.13	0.36	0.19	0.04	0.18
P	0.79	0.24	0.12	0.15	0.95	0.38	0.08

Note: GMI—Garwood massive ice; the number indicates the depth below the surface at which the sample was collected (see Fig. 2 for sampling area). *P*—probability that JLI samples and GMI samples are derived from same ice compositional population based on single-ended analysis of variance. No values are significantly different ($P < 0.05$), suggesting a relatively homogeneous ion load in Garwood Valley ice.

TABLE 6. SUMMARY OF CARBONATE ISOTOPIC COMPOSITIONS BASED ON DI-IRMS

Sample	$\delta^{13}\text{C}$ (‰, VPDB)	$\delta^{18}\text{O}$ (‰, VPDB)	Carbonate (wt%)
G11A	2.68 ± 0.01	-12.93 ± 0.14	9.2 ± 0.4
G11B	2.56 ± 0.01	-15.33 ± 0.14	10.7 ± 0.4
G14	3.49 ± 0.01	-19.41 ± 0.14	14.1 ± 0.4
G14A	2.98 ± 0.01	-16.37 ± 0.14	14.5 ± 0.4
G20	2.41 ± 0.01	-11.38 ± 0.14	3.0 ± 0.4

Note: Error is standard deviation of repeat measurements. DI-IRMS—dual-inlet isotope ratio mass spectrometer; VPDB—Vienna Pee Dee belemnite.

of Garwood Valley and the ice located at the ice cliff and beneath the delta complex. Compositionally, the upper valley ice and the lower valley ice are nearly identical. Nevertheless, single-ended ANOVA analyses of the O and H isotopic values (‰ Vienna standard mean ocean water [VSMOW]) of the two ices yield significant differences: Ice from the ice cliff area is significantly more depleted in D than down-valley ice (-241‰ vs. -219‰, $P < 0.002$) and is also significantly more depleted in ^{18}O than down-valley ice (-30‰ vs. -27‰, $P < 0.01$). These data suggest that, while the buried Ross Sea ice sheet in Garwood Valley is compositionally homogeneous, it records a complex isotopic history of similar complexity to the modern Ross Ice Shelf (Kellogg et al., 1990), which reflects intermingled ice sources reflecting both marine and glacial origins. It is also possible that thermal and physical erosion by the Garwood River through the stranded Ross Sea ice sheet lobe of buried ice has resulted in the intermingling of locally derived ice (transported as river meltwater and refrozen in place) with Ross Sea ice sheet ice, which could account for the similarity in isotopic values between some ice-cliff ice and the Garwood Glacier.

Next, how does the isotopic composition of Garwood Valley carbonates compare to those from neighboring Miers Valley, and what does that indicate about the water sources for the paleolakes in which these carbonates formed? Clayton-Greene et al. (1988) reported calcium carbonate $\delta^{18}\text{O}$ and $\delta^{13}\text{C}$ values spanning ~-33‰ to -19‰ and 3.5‰ to 6.5‰, respectively (all ratios in this paragraph are Vienna Pee Dee belemnite [VPDB]), similar to values reported for Glacial Lake Washburn (in Taylor Valley) by Lawrence and Hendy (1989): ~-30‰ to -17‰ for $\delta^{18}\text{O}$ and ~-4‰ to +4‰ for $\delta^{13}\text{C}$. Clayton-Greene et al. (1988) interpreted these relatively enriched $\delta^{18}\text{O}$ values (relative to buried ice or ice-sheet values) as evidence of local, meteoric sources (e.g., alpine glaciers), rather than melting of distantly formed ice-sheet ice as the primary source for Miers Valley lake waters. Garwood Valley carbonates sampled from the delta complex and measured at the Oregon State University College of Earth, Ocean, and Atmospheric Sciences Stable Isotope Labora-

tory on a Kiel III/MAT25 DI-IRMS are broadly similar to these paleolake carbonates, with $\delta^{18}\text{O}$ values spanning ~-19‰ to -11‰ and $\delta^{13}\text{C}$ values spanning ~-2.4‰ to -3.5‰ (Table 6). Taken together, this suite of oxygen isotopic values is consistent with the Clayton-Greene et al. (1988) model of southern McMurdo Dry Valleys filling with the locally derived meltwater after ice damming by the Ross Sea ice sheet. Flow of glacial runoff and snowmelt in the McMurdo Dry Valleys typically results in evaporation and enrichment of streamflow in heavy ^{18}O , relative to the meteoric sources (Fig. 18) (Gooseff et al., 2006), and it is likely that the paleo-Garwood River behaved similarly to its modern counterpart.

Finally, how does the mineralogical composition of carbonate-bearing units in Garwood Valley compare to the composition of analogous units in Miers and Marshall Valleys, and what does that indicate about the dehydration history of Glacial Lake Howard? Miers and Marshall Valleys both contain diagnostic mineral assemblages containing mixed carbonates (calcite and aragonite) and thick gypsum beds, which have been interpreted as evidence of evaporation of the ice-sheet-dammed paleolakes present in those valleys during LGM time (Clayton-Greene et al., 1988; Dage, 1985). Garwood Valley delta complex samples interpreted as lacustrine bottomset deposits (G11B, G20, G14, G14A, G11A, and G18) were analyzed using a Philips XRG 3100 Automated X-ray Diffractometer at Oregon State University. Powders of the samples were prepared by gently disaggregating the samples in an agate mortar. All samples contained carbonates, with the exception of G18. Only calcite was found in the Garwood Valley samples, based on the diagnostic diffraction lines identified using the JADE search/match software. No gypsum, nor aragonite, was identified. We interpret these results to indicate that the Garwood Valley paleolake (Glacial Lake Howard) did not desiccate; rather, the drawdown of the lake level required to produce the stepped delta complex was accomplished by lake drainage through the ice plug at the mouth of the valley. We interpret the carbonates to be of biogenic origin, and to have settled to the lakebed in a manner comparable with modern McMurdo Dry Valleys lake environments, in

which thick carbonate accumulations are produced through seasonal algal/planktonic activity (Vopel and Hawes, 2006; Sutherland and Hawes, 2009).

In summary, geochemical analyses of Garwood Valley sediments and ices indicate that they are broadly similar to LGM-era sediment and ice deposits found in neighboring valleys. All experienced similar ice damming and paleolake development driven by local ice melt and evaporative enrichment of source waters. Differences in lake history (desiccation in Miers vs. continuity in Garwood) are reflected in the mineralogical record in the valleys. In addition, spatial sampling of ice deposits in Garwood suggests that an age record of Ross Sea ice sheet stable isotope variability may be preserved laterally in the ice buried beneath the down-valley (and possibly up-valley) till.

CONCLUSIONS

Ice and sediment deposits in Garwood Valley provide a new perspective on the timing of transitions between Pleistocene and Holocene glaciofluvial conditions in the southern McMurdo Dry Valleys. Deposition in the Garwood Valley proglacial lake (Glacial Lake Howard) persisted from at least 26 ka, when the lake was formed by damming of the valley by Ross Sea ice sheet ice, to ca. 5.5 ka, when retreat of the Ross Sea ice sheet grounding line past the mouth of the valley permitted the sequential draining of the lake into the Ross Sea starting at ca. 7.3 ka.

This ~20 k.y. history of activity is recorded in a single outcrop in Garwood Valley (the delta complex), making it an unusually complete chronostratigraphic sequence in the McMurdo Dry Valleys. Most unusually, the Garwood paleodelta outcrops sit conformably atop intact glacial till units, which in turn overlie buried massive ice deposits interpreted to be remnants of the stranded Ross Sea ice sheet emplaced in the valley during the late Pleistocene. Strikingly, the Garwood Valley delta complex and associated glaciofluvial landforms indicate that the particular geological and hydrological conditions in Garwood Valley permitted growth of a very large delta in a very small ice-dammed lake.

After initial lake formation, the earliest deposition of sediments in Glacial Lake Howard is associated with local maxima in the $\delta^{18}\text{O}$ ice-core record at the nearby Taylor Dome, indicating deposition during periods of relative warmth in the McMurdo Dry Valleys, even during broadly colder periods during the late Pleistocene. Deposition of the complex topset/foreset units in the delta was not strongly associated with particular Taylor Dome climate modes, suggesting

complex interplay between climate and local McMurdo Dry Valleys hydrometeorology.

Glacial Lake Howard shows no evidence of complete dehydration, and rather, it is interpreted to have largely drained through breaching of the ice dam in the mouth of the valley. No gypsum plates exist in the Garwood Valley paleodelta. Likewise, subaerial sedimentary markers (remnant sand wedges) are only observed in the oldest glacial till unit immediately overlying the buried ice, and not in any other stratigraphic unit, suggesting persistent lacustrine conditions without intervening subaerial periods.

Garwood Valley ice and sediment geochemical and isotopic compositions are broadly consistent with carbonate and ice compositions recorded elsewhere in the Ross Sea (Ross I) drift. Buried glacial ice is geochemically homogeneous within Garwood Valley, but it shows stable isotope variability that may indicate the presence of a horizontally distributed climate record. Garwood Valley lacustrine carbonate oxygen and carbon compositions are most consistent with lake formation dominated by the proximal melting of alpine glaciers, with minimal contributions from melting of the ice-sheet dam.

Chronostratigraphic and geochemical analyses of glaciofluvial units in Garwood Valley result in observations and inferences that are broadly consistent with glacial reconstructions conducted elsewhere in the McMurdo Dry Valleys. Garwood Valley is unique, however, in the complexity and detail of the sedimentary record preserved from the Pleistocene-Holocene transition, and in the richness of the delta complex outcrop for conducting future studies of paleo-hydrology in Antarctica during the close of the last ice age.

ACKNOWLEDGMENTS

This work was supported by the U.S. National Science Foundation (NSF) Antarctic Earth Sciences program under award ANT-1212307 to Levy, Fountain, and Lyons. Many thanks go to the extensive team that made this research possible, notably, to Captain Dustin Black for bringing the Garwood Valley ice cliff to the attention of the research team, and to all the PHI pilots and ground staff for providing reliable and safe access to the site; to Thomas Nylen, Hasan Basagic, James Dickson, Rickard Pettersson, and James Jerome Bethune for field assistance; to Deb Leslie for stable isotope analyses of ice samples; to Jennifer McKay for stable isotope analysis of Garwood carbonates; to the Arizona Accelerator Mass Spectrometry (AMS) Laboratory for radiocarbon dating services; to Paul Morin and the Polar Geospatial Center for access to satellite image data; and to John Dilles, Federico Cernushi, Matt Lowen, and Mark Ford for assistance in X-ray diffraction analysis of sediments. Light detection and ranging (LIDAR) topography used in this paper was kindly made pos-

sible through a joint effort from the NSF, the National Aeronautics and Space Administration, and the U.S. Geological Survey, with basic postprocessing from the Byrd Polar Research Center. This manuscript has benefited from thoughtful reviews from Brenda Hall, and two anonymous reviewers.

REFERENCES CITED

- Bindschadler, R., Vornberger, P., Flemming, A., Fox, A., Mullins, J., Binnie, D., Paulsen, S.J., Granneman, B., and Gorodetzky, D., 2008, The Landsat image mosaic of Antarctica: Remote Sensing of Environment, v. 112, no. 4, p. 4214–4226.
- Brook, E.J., Brown, E.T., Kurz, M.D., Ackert, R.P., Raisbeck, G.M., and Yiou, F., 1995, Constraints on age, erosion, and uplift of Neogene glacial deposits in the Transantarctic Mountains determined from in situ cosmogenic ^{10}Be and ^{26}Al : *Geology*, v. 23, p. 1063–1066, doi:10.1130/0091-7613(1995)023<1063:COAEAU>2.3.CO;2.
- Clayton-Greene, J.M., and Hendy, C.H., 1987, The origin of drift mounds in Miers Valley, Antarctica: *Antarctic Journal of the United States*, v. 22, no. 3, p. 59–60.
- Clayton-Greene, J.M., Hendy, C.H., and Hogg, A.G., 1988, Chronology of a Wisconsin age proglacial lake in the Miers Valley, Antarctica: *New Zealand Journal of Geology and Geophysics*, v. 31, p. 353–361, doi:10.1080/00288306.1988.10417781.
- Conway, H., Hall, B.L., Denton, G.H., Gades, A.M., and Waddington, E.D., 1999, Past and future grounding-line retreat of the West Antarctic Ice Sheet: *Science*, v. 286, p. 280–283, doi:10.1126/science.286.5438.280.
- Dagel, M.A., 1985, Stratigraphy and Chronology of State 6 and 2 Glacial Deposits, Marshall Valley, Antarctica [M.S. thesis]: Orono, Maine, University of Maine, 82 p.
- Denton, G.H., and Marchant, D.R., 2000, The geological basis for a reconstruction of a grounded ice sheet in the McMurdo Sound, Antarctica, at the Last Glacial Maximum: *Geografiska Annaler*, ser. A, v. 82, no. 2/3, p. 167–211.
- Denton, G.H., Bockheim, J.G., Wilson, S.C., and Stuiver, M., 1989, Late Wisconsin and early Holocene glacial history, Inner Ross embayment, Antarctica: *Quaternary Research*, v. 31, p. 151–182, doi:10.1016/0033-5894(89)90004-5.
- Doran, P.T., Wharton, R., and Lyons, W.B., 1994, Paleolimnology of the McMurdo Dry Valleys: *Journal of Paleolimnology*, v. 10, no. 2, p. 85–114, doi:10.1007/BF00682507.
- Doran, P.T., McKay, C.P., Fountain, A.G., Nylen, T., McKnight, D.M., Jaros, C., and Barrett, J.E., 2008, Hydrologic response to extreme warm and cold summers in the McMurdo Dry Valleys, East Antarctica: *Antarctic Science*, v. 20, p. 499–509, doi:10.1017/S0954102008001272.
- Fairbanks, R.G., Mortlock, R.A., Chiu, T.-Z., Cao, L., Kaplan, A., Guilderson, T.P., Fairbanks, T.W., and Bloom, A.L., 2005, Marine radiocarbon calibration curve spanning 0 to 50,000 years B.P. based on paired $^{230}\text{Th}/^{234}\text{U}$ and ^{14}C dates on pristine corals: *Quaternary Science Reviews*, v. 24, p. 1781–1796, doi:10.1016/j.quascirev.2005.04.007.
- Gooseff, M.N., Lyons, W.B., McKnight, D.M., Vaughn, B.H., Fountain, A.F., and Dowling, C., 2006, A stable isotopic investigation of a polar desert hydrologic system, McMurdo Dry Valleys, Antarctica: *Arctic, Antarctic, and Alpine Research*, v. 38, no. 1, p. 60–71, doi:10.1657/1523-0430(2006)038[0060:ASIOAJ]2.0.CO;2.
- Hall, B.L., and Denton, G.H., 2000, Radiocarbon chronology of Ross Sea Drift, eastern Taylor Valley, Antarctica: Evidence for a grounded ice sheet in the Ross Sea at the Last Glacial Maximum: *Geografiska Annaler*, ser. A, v. 82, no. 2–3, p. 305–336.
- Hall, B.L., and Denton, G.H., 2005, Surficial geology and geomorphology of eastern and central Wright Valley, Antarctica: *Geomorphology*, v. 64, p. 25–65, doi:10.1016/j.geomorph.2004.05.002.
- Hall, B.L., and Henderson, G.M., 2001, Use of uranium–thorium dating to determine past ^{14}C reservoir effects in lakes: Examples from Antarctica: *Earth and Planetary Science Letters*, v. 193, no. 3, p. 565–577.
- Hall, B.L., Denton, G.H., and Hendy, C.H., 2000, Evidence from Taylor Valley for a grounded ice sheet in the Ross Sea, Antarctica: *Geografiska Annaler*, ser. A, v. 82, no. 2–3, p. 275–303.
- Hall, B.L., Hendy, C.H., and Denton, G.H., 2006, Lake-ice conveyor deposits: Geomorphology, sedimentology, and importance in reconstructing the glacial history of the Dry Valley: *Geomorphology*, v. 75, p. 143–156, doi:10.1016/j.geomorph.2004.11.025.
- Hall, B.L., Denton, G.H., Overturf, B., and Hendy, C.H., 2002, Glacial Lake Victoria, a high-level Antarctic lake inferred from lacustrine deposits in Victoria Valley: *Journal of Quaternary Science*, v. 17, no. 7, p. 697–706, doi:10.1002/jqs.691.
- Hall, B.L., Baroni, C., and Denton, G.H., 2004, Holocene relative sea-level history of the southern Victoria Land Coast, Antarctica: *Global and Planetary Change*, v. 42, no. 1–4, p. 241–263, doi:10.1016/j.gloplacha.2003.09.004.
- Hall, B.L., Denton, G.H., Fountain, A.G., Hendy, C.H., and Henderson, G.M., 2010, Antarctic lakes suggest millennial reorganizations of Southern Hemisphere atmospheric and oceanic circulation: *Proceedings of the National Academy of Sciences of the United States of America*, v. 107, no. 50, p. 21,355–21,359, doi:10.1073/pnas.1007250107.
- Hendy, C.H., 2000, Quaternary lakes in the McMurdo Sound region of Antarctica: *Geografiska Annaler*, ser. A, v. 82, no. 2–3, p. 411–432.
- Hendy, C.H., and Hall, B.L., 2006, The radiocarbon reservoir effect in proglacial lakes: Examples from Antarctica: *Earth and Planetary Science Letters*, v. 241, p. 413–421, doi:10.1016/j.epsl.2005.11.045.
- Hendy, C.H., Healy, T.R., Rayner, E.M., Shaw, J., and Wilson, A.T., 1979, Late Pleistocene glacial chronology of the Taylor Valley, Antarctica, and the global climate: *Quaternary Research*, v. 11, p. 172–184, doi:10.1016/0033-5894(79)90002-4.
- Higgins, S.M., Hendy, C.H., and Denton, G.H., 2000, Geochronology of Bonney Drift, Taylor Valley, Antarctica: Evidence for interglacial expansions of Taylor Glacier: *Geografiska Annaler*, ser. A, v. 82, no. 2–3, p. 391–409.
- Hoffman, M.J., Fountain, A.G., and Liston, G.E., 2008, Surface energy balance and melt thresholds over 11 years at Taylor Glacier, East Antarctica: *Journal of Geophysical Research*, v. 113, F04014, doi:10.1029/2008JF001029.
- Joy, K., Carson, N., Fink, D., and Storey, B., 2011, In-situ cosmogenic exposure dating in the Miers and Garwood Valleys, Denton Hills, Antarctica, in 12th International Conference on Accelerator Mass Spectrometry: Wellington, New Zealand, abstract GLO#16, p. 144.
- Kellogg, T.B., Kellogg, D.F., and Stuiver, M., 1990, Late Quaternary history of the southwestern Ross Sea: Evidence from debris bands on the McMurdo Ice Shelf, Antarctica, in Bentley, C.R., ed., *Contributions to Antarctic Research*: Washington, D.C., American Geophysical Union, p. 73–76.
- Lawrence, M.J.F., and Hendy, C.H., 1989, Carbonate deposition and Ross Sea ice advance, Fryxell basin, Taylor Valley, Antarctica: *New Zealand Journal of Geology and Geophysics*, v. 32, no. 2, p. 267–278, doi:10.1080/00288306.1989.10427588.
- Marchant, D.R., Lewis, A.R., Phillips, W.M., Moore, E.J., Souchez, R.A., Denton, G.H., Sugden, D.E., Potter, N.J., and Landis, G.P., 2002, Formation of patterned ground and sublimation till over Miocene glacier ice in Beacon Valley, southern Victoria Land, Antarctica: *Geological Society of America Bulletin*, v. 114, no. 6, p. 718–730, doi:10.1130/0016-7606(2002)114<0718:FOPGAS>2.0.CO;2.
- Péwé, T.L., 1960, Multiple glaciations in the McMurdo Sound region, Antarctica: A progress report: *The Journal of Geology*, v. 68, no. 5, p. 498–514, doi:10.1086/626684.
- Pollard, W., Doran, P., and Wharton, R., 2002, The nature and significance of massive ground ice in Ross Sea Drift, Garwood Valley, McMurdo Sound: *Royal Society of New Zealand Bulletin*, v. 35, p. 397–404.
- Prentice, M.L., Arcone, S.A., Curren, M.G., Delaney, A.J., Horsman, J., Letsinger, S.L., Medley, E.A., and Gaynor, J.R., 2008, Stratigraphy and geomorphology of late Pleistocene moraine at the mouth of Taylor Valley, Antarctica: Implications for the melting history of the West

- Antarctic Ice Sheet during the last deglaciation: San Francisco, California, American Geophysical Union Fall Meeting, abstract C31C-0504.
- Reimer, P.J., Baillie, M.G.L., Bard, E., Bayliss, A., Beck, J.W., Blackwell, P.G., Ramsey, C.B., Buck, C.E., Burr, G.S., and Edwards, R.L., 2009, IntCal09 and Marine09 radiocarbon age calibration curves, 0–50,000 years cal BP: *Radiocarbon*, v. 51, no. 4, p. 1111–1150.
- Richter, I., 2011, Influences of Soil Properties on Archaeal Diversity and Distribution in the McMurdo Dry Valleys, Antarctica [Sc.M. thesis]: Hamilton, New Zealand, University of Waikato, 138 p.
- Schenk, T., Csatho, B.M., Ahn, Y., Yoon, T., and Shin, W.S., 2004, DEM Generation from the Antarctic LiDAR Data: Site Report: U.S. Geological Survey, http://usarc.usgs.gov/lidar/lidar_pdfs/Site_reports_v5.pdf (accessed January 2012).
- Steig, E.J., Morse, D.L., Waddington, E.D., Stuiver, M., Grootes, P.M., Mayewski, P.A., Twickler, M.S., and Whitlow, S.I., 2000, Wisconsinan and Holocene climate history from an ice core at Taylor Dome, western Ross Embayment, Antarctica: *Geografiska Annaler*, ser. A, v. 82, no. 2–3, p. 213–235.
- Stuiver, M., and Reimer, P.J., 1993, Extended ^{14}C database and revised CALIB 3.0 ^{14}C age calibration program: *Radiocarbon*, v. 35, no. 1, p. 215–230.
- Stuiver, M., Denton, G.H., Hughes, T., and Fastook, J.L., 1981, History of the marine ice sheet in West Antarctica during the last glaciation: A working hypothesis, in Denton, G.H., and Hughes, T., eds., *The Last Great Ice Sheets*: New York, John Wiley and Sons, p. 319–436.
- Sugden, D.E., Marchant, D.R., and Denton, G.H., 1993, The case for a stable East Antarctic Ice Sheet: The background: *Geografiska Annaler*, ser. A, v. 75, no. 4, p. 151–154, doi:10.2307/521199.
- Sutherland, D., and Hawes, I., 2009, Annual growth layers as proxies of past growth conditions for benthic microbial mats in a perennially ice-covered, Antarctic lake: *FEMS Microbial Ecology*, v. 67, p. 279–272.
- Vopel, K., and Hawes, I., 2006, Photosynthetic performance of benthic microbial mats in Lake Hoare, Antarctica: *Limnology and Oceanography*, v. 51, p. 1801–1812, doi:10.4319/lo.2006.51.4.1801.
- Welch, K.A., Lyons, W.B., Whisner, C., Gardner, C.B., Gooseff, M.N., McKnight, D.M., and Priscu, J.C., 2010, Spatial variations in the geochemistry of glacial meltwater streams in Taylor Valley, Antarctica: *Antarctic Science*, v. 22, no. 6, p. 662–672, doi:10.1017/S0954102010000702.

SCIENCE EDITOR: CHRISTIAN KOEBERL
ASSOCIATE EDITOR: BENJAMIN J.C. LAABS

MANUSCRIPT RECEIVED 2 SEPTEMBER 2012
REVISED MANUSCRIPT RECEIVED 4 MARCH 2013
MANUSCRIPT ACCEPTED 5 MARCH 2013

Printed in the USA